

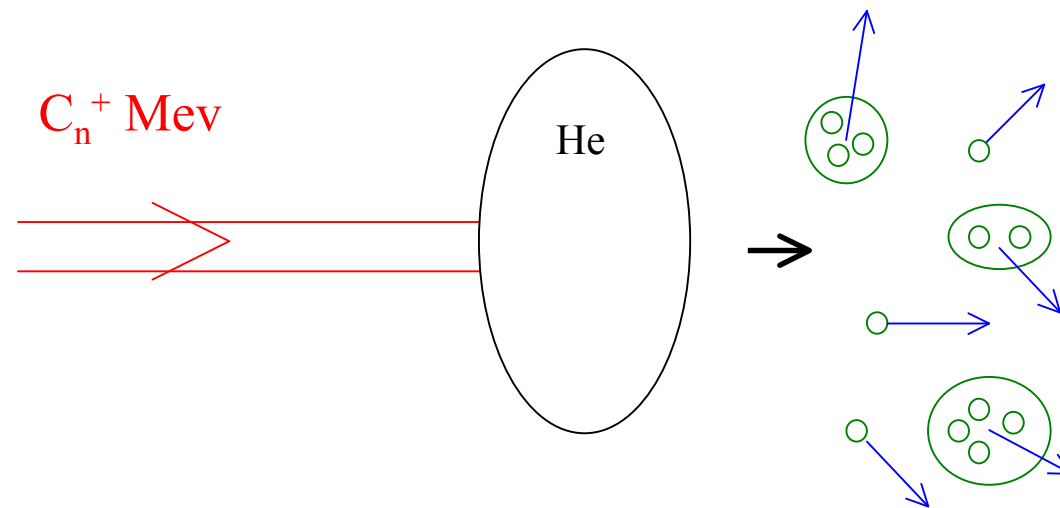
Statistical Fragmentation of Atomic Clusters

CCSD(T)/6-311+G(3df)

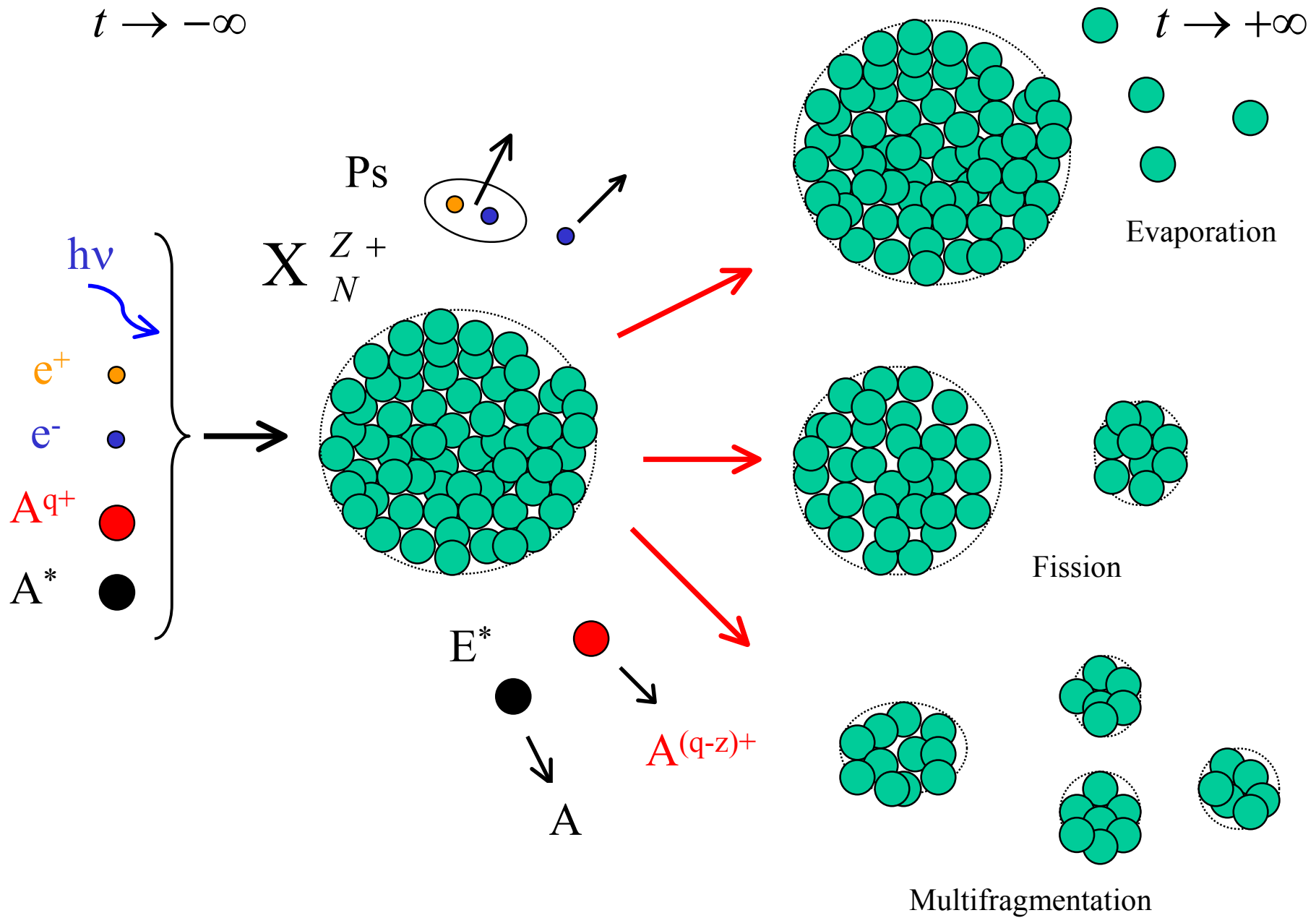
P. -A. Hervieux

IPCMS, University of Strasbourg

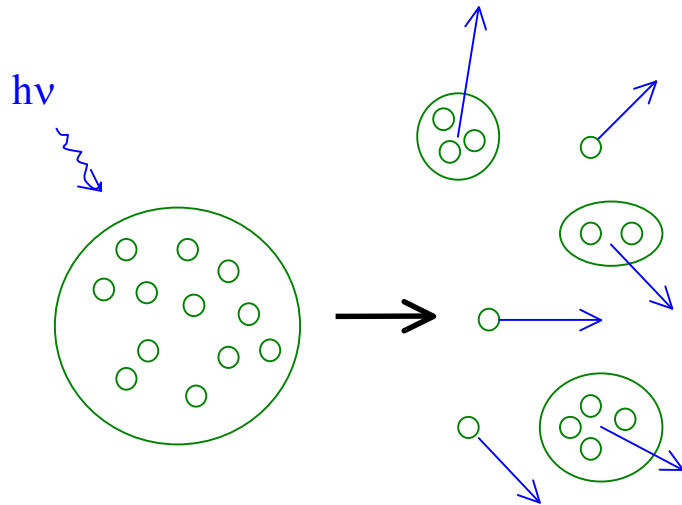
MMMC
Weisskopf



IPN-14/03/05

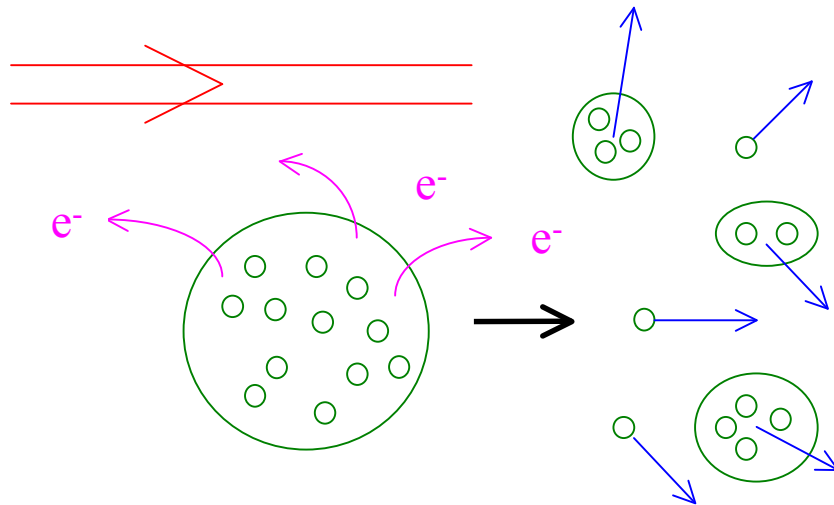


How to break up a cluster ? (1)



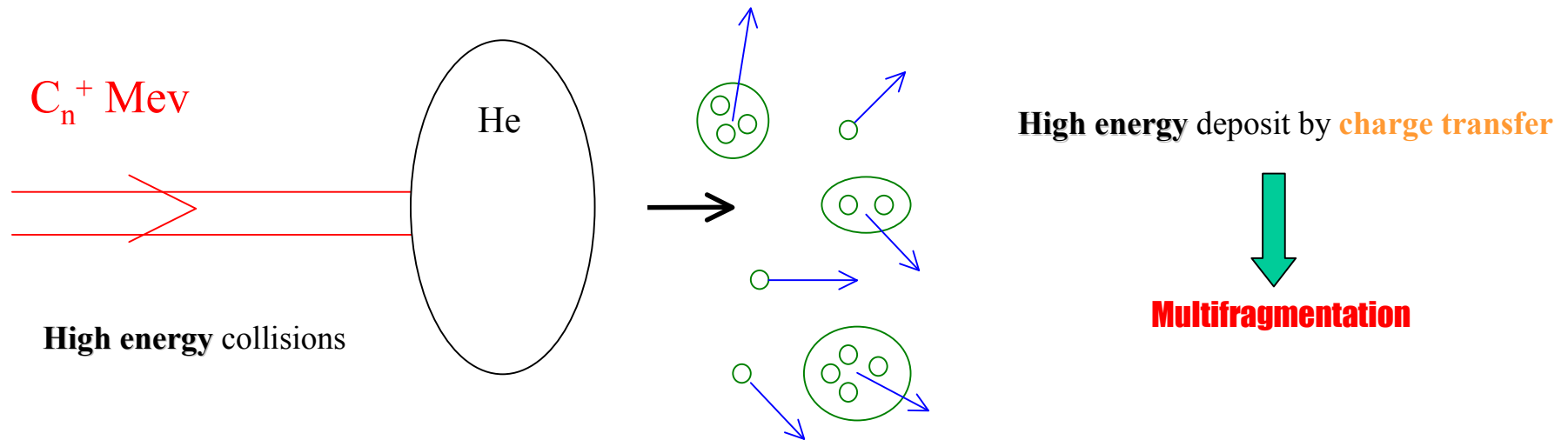
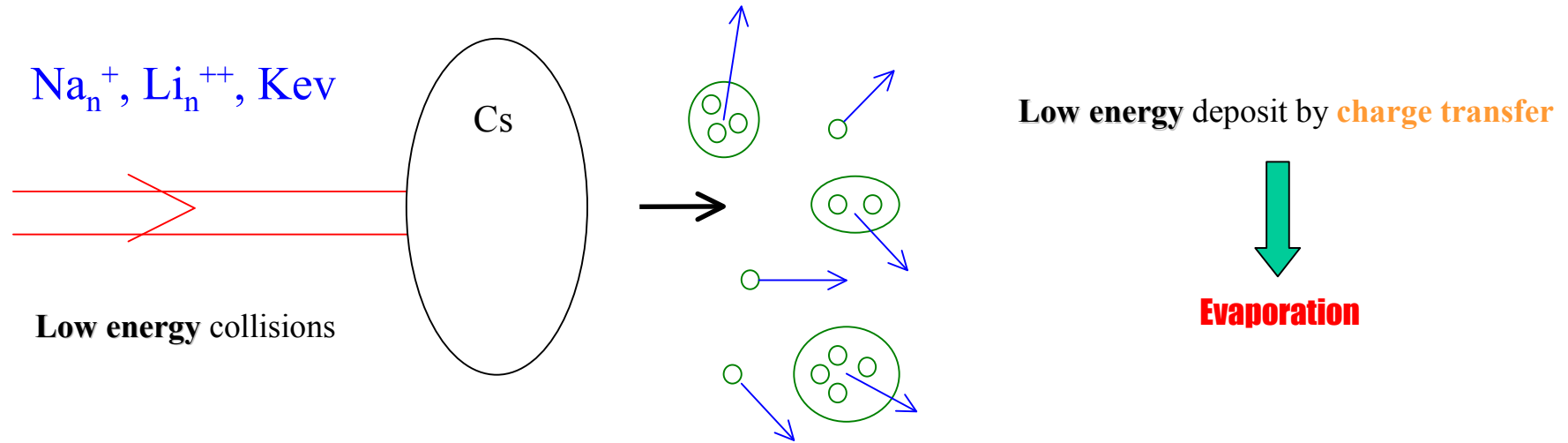
Multiphoton absorption
(energy excess)

A^{q+}

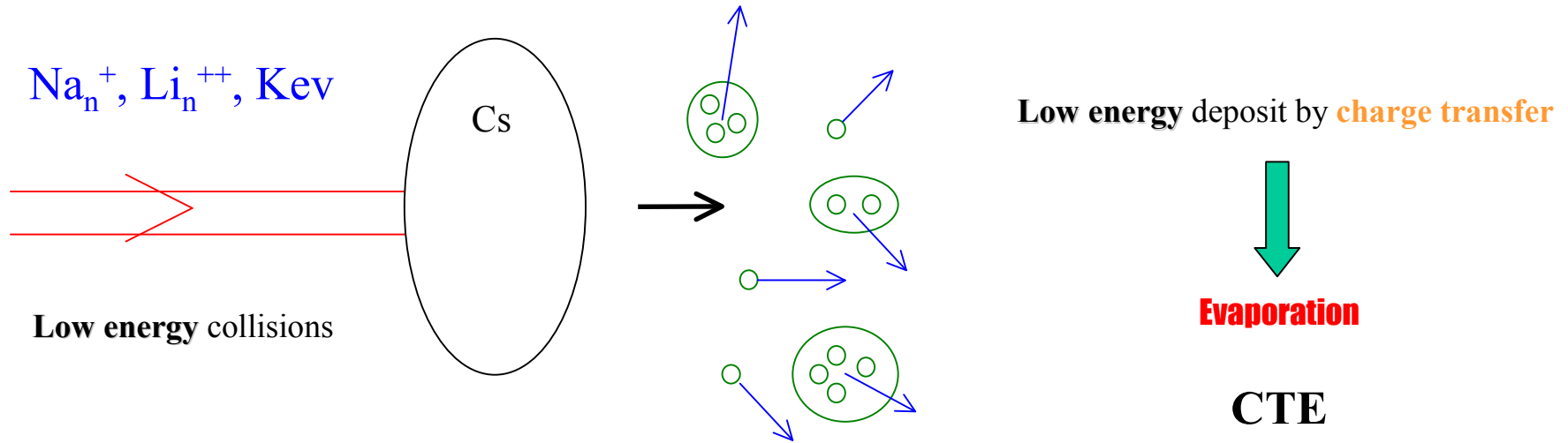


Coulomb explosion
(charge excess)

How to break up a cluster ? (2)

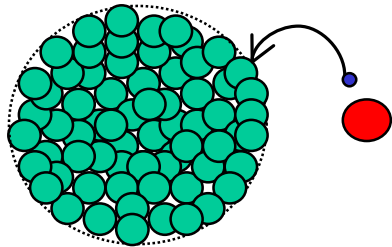


Low Energy Fragmentation



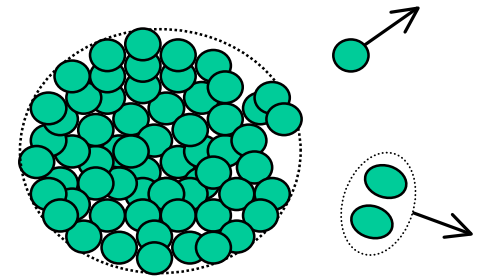
Part I

Charge Transfer and Evaporation in Low Energy Collisions of Metal Clusters and Fullerenes with Atomic Targets



P. -A. Hervieux

IPCMS, University of Strasbourg



F. Martín, M. Alcamí, S. Díaz-Tendero and L. F. Ruiz

Departamento de Química, University of Madrid, Spain

M. F. Politis

G.P.S., University of Paris VII, France

J. Hanssen and B. Zarour

L.P.M.C., University of Metz, France

Motivations

➔ **Metal Clusters** are the **ideal tool** to bridge the gap between *molecules* and *surfaces*

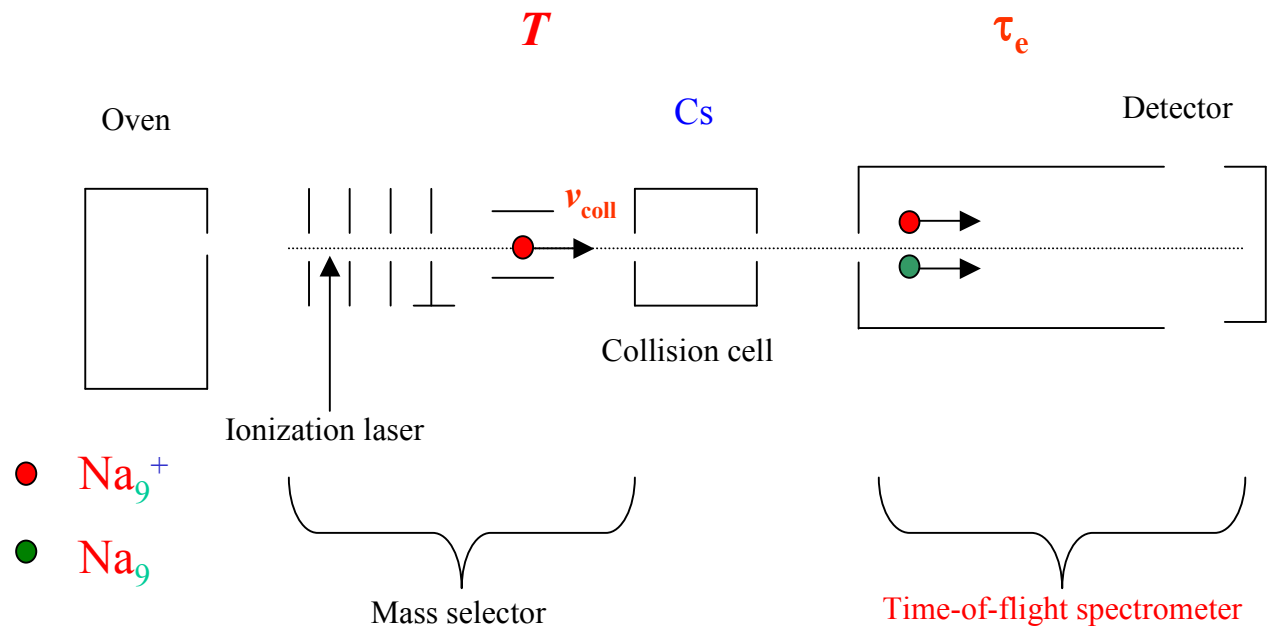
➔ **Theoretical challenge**: study of a **complex collision process** involving a **lot of electronic and nuclear degrees of freedom**

From $t = -\infty$ to $t = +\infty$

➔ Experimental measurements are available

C. Bréchnac et al. *Eur. Phys. J. D* **12**, 185 (2000); **16**, 91 (2001)

Experimental Setup (LAC-Orsay)



Time Scales

★ **Experiment:** $v_{\text{coll}} \sim 0.01 - 0.07 \text{ a.u.} \rightarrow \tau_{\text{coll}} \sim 10^{-14} \text{ s}$

★ **Cluster vibrational period:** $\tau_v \sim 10^{-12} \text{ s}$
internal motion of the cluster nuclei



$$\tau_v \gg \tau_{\text{coll}}$$

Ionic background of the cluster is frozen during the collision

★ **Electron-phonon coupling:** $\tau_{\text{rel}} \sim 10^{-13} - 10^{-12} \text{ s}$

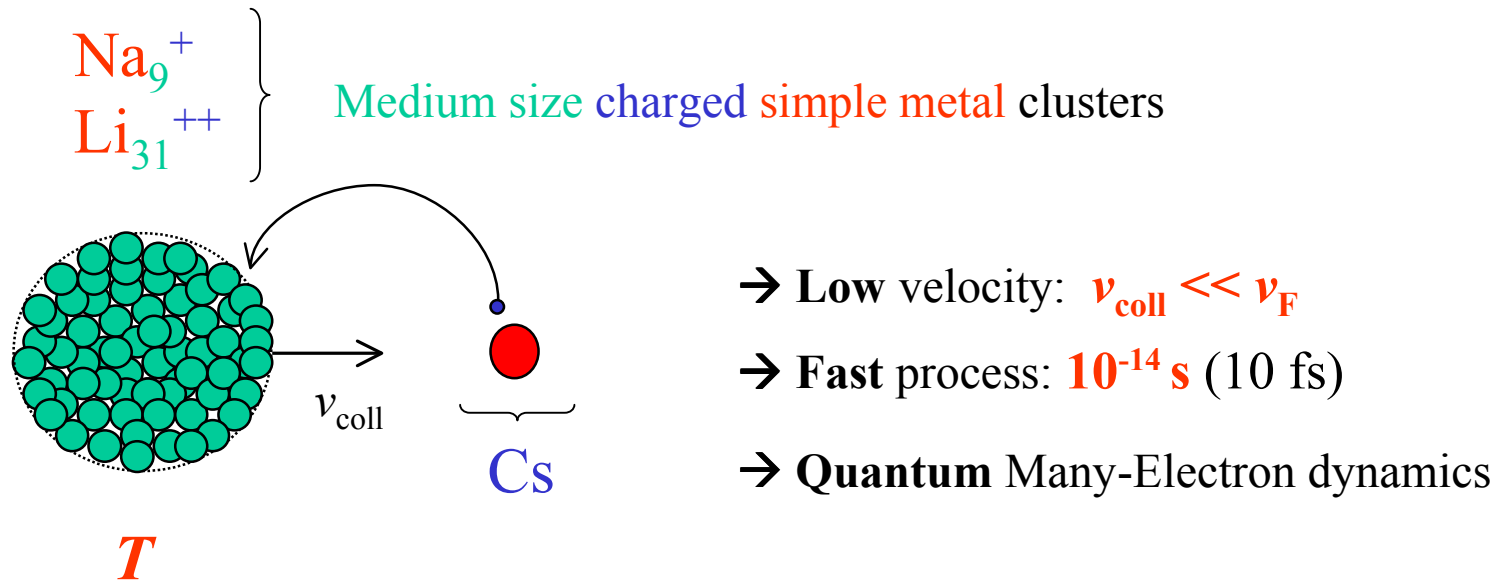


$$\tau_{\text{rel}} \gg \tau_{\text{coll}}$$

*Dissociation processes resulting from electronic relaxation
can be ignored during the collision*

★ *Collision and fragmentation can be treated separately*

First Step (Fast)

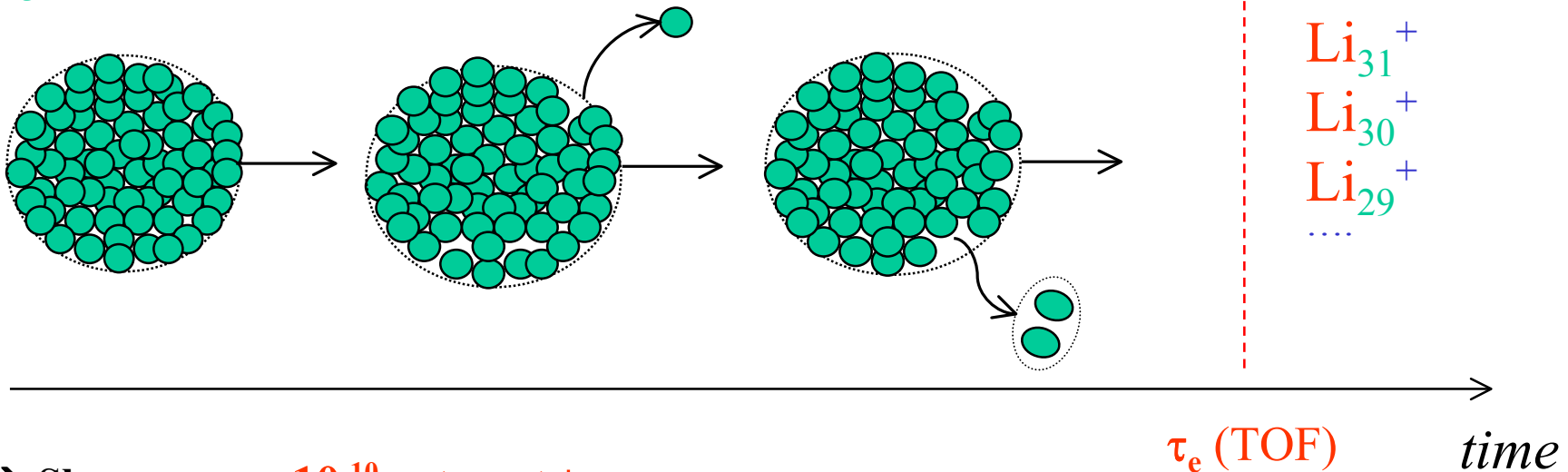


Charge Transfer (CT) \rightarrow **Inclusive Cross-section**

Second Step (Slow)

Na_9^* (neutrals)

Li_{31}^{+*} (charged)



→ Slow process: $10^{-10} \text{ s} < \tau_{\text{fr}} < +\infty$

→ Classical Many-Ion dynamics

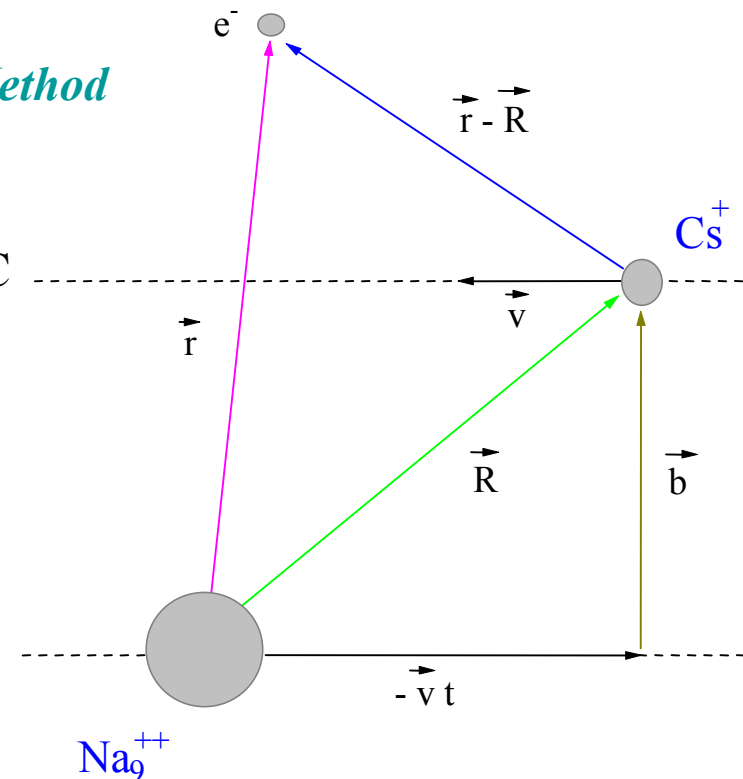
→ Sequential evaporation of monomer or dimer

Charge-transfer induced evaporation (CTE) →

Exclusive cross-sections
Fragmentation cross sections

Electron Dynamics

- **Valence electrons** → fully quantum mechanical description
- **Nuclei** → classical description
- $v_{\text{coll}} \ll v_F \sim 0.53 \text{ a.u. (Cs)}$ → *Molecular Method*
- **Cluster Electronic Ground-State**
→ Spherical Jellium Model + DFT-LDAXC-SIC
- **Collision**
→ Time-Dependent Molecular Close-Coupling
→ Impact parameter method
- **Many-electron Dynamics**
→ Inclusive Probabilities Formalism
(Independent Electron Model)



M. F. Politis et al., Phys. Rev. A **58**, 367 (1998); F. Martín et al., Phys. Rev. B **58**, 6752 (1998)

Energy Deposit

Collision $\rightarrow E_{coll}^*(b) \rightarrow$ Fragmentation

$$E_{coll}^*(b) = \left\langle \Psi_{f_1, \dots, f_{N_e}} \left| \hat{H} - E_0 \right| \Psi_{f_1, \dots, f_{N_e}} \right\rangle$$

- ★ One must add the **thermal energy** of the cluster before the collision: E_T^*
T is the vibrational temperature
- ★ Obtained from the **specific heat at constant pressure** of the **bulk**

$$\varepsilon(T) \cong h(T) - h_0 = \int_0^T C_p(T) dT = E_T^* / N$$

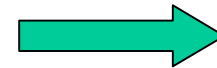
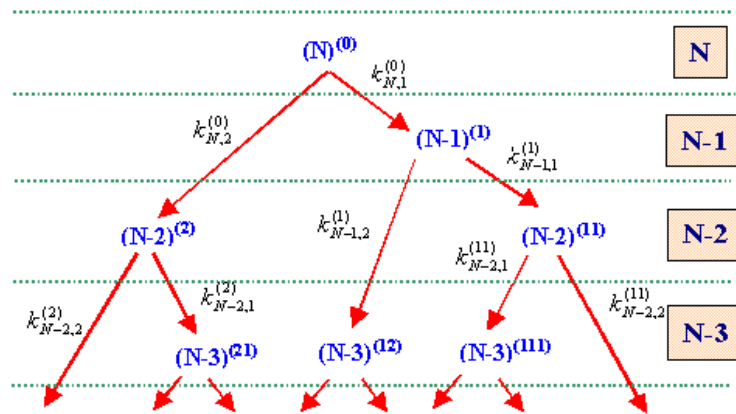
- ★ **Total vibrational excitation energy** $E^*(b) = E_{coll}^*(b) + E_T^*$

Fragmentation Dynamics

Sequential Evaporation Model

P. -A. Hervieux et al.,
J. Phys. B 34, 3331 (2001)

- ★ Includes **Monomer** and **Dimer** Evaporation to any order



$$\left\{ \begin{array}{l} \frac{dn_N^{(0)}}{dt} = -k_N^{(0)} n_N^{(0)} \\ \frac{dn_{N-1}^{(1)}}{dt} = -k_{N-1}^{(0)} n_N^{(0)} - k_{N-1}^{(1)} n_{N-1}^{(1)} \\ \frac{dn_{N-2}^{(2)}}{dt} = -k_{N-2}^{(0)} n_N^{(0)} - k_{N-2}^{(2)} n_{N-2}^{(2)} \\ \frac{dn_{N-2}^{(11)}}{dt} = -k_{N-1,1}^{(1)} n_{N-1}^{(1)} - k_{N-2}^{(11)} n_{N-2}^{(11)} \\ \dots \end{array} \right.$$

Time integration stops at $t = \tau_e$

- ★ **Rate constants:** Microscopic and Microcanonical Statistical theory of Weisskopf
- ★ Entropy of the **bulk** and binding energies from the **experiment**

$$\left. \begin{array}{l} P_{ev,j}(b) = \frac{n_{n-j}(\tau_e)}{N^{(0)}} \\ P_{Na_{9-i}}(b) = P^{CT}(b) \times P_{ev,i}(b) \end{array} \right\} \longrightarrow \underbrace{\sigma_\alpha = 2\pi \cdot \int_{R_C}^{\infty} b \cdot P_\alpha(b) db}_{\text{Fragmentation cross sections}}$$

Fragmentation cross sections

Rates of Evaporation Theory of Weisskopf (RRKM)

Fragmentation of the ionic background

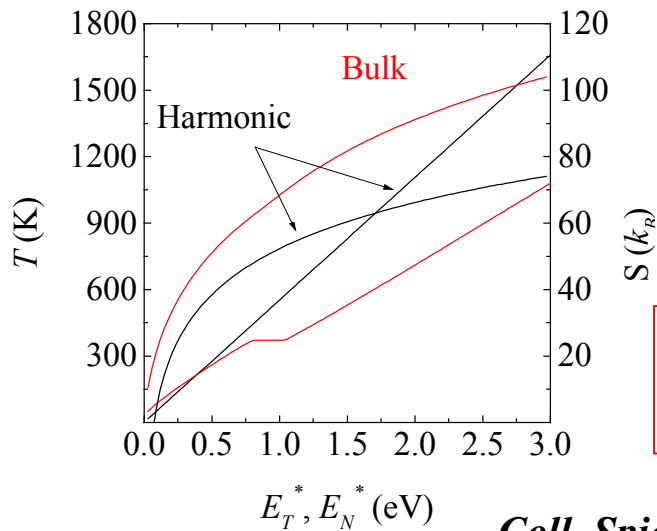
→ Microscopic and Microcanonical Statistical model

$$\frac{dN_{if}}{dt} = \frac{2\pi}{\hbar} |M_{if}|^2 \rho_f(E_N^*)$$

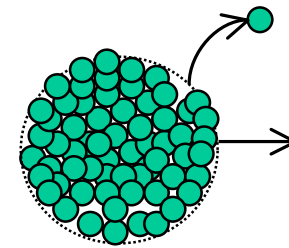
with $\rho_f(E_N^*) = \int_0^{E_N^* - D_{N,1}} \rho_1^t(e) \rho_{N-1}^v(E_N^* - D_{N,1} - e) de$

→ From *experimental* C_p of the bulk

$$\left\{ \begin{array}{l} s(T) = \int_0^T \frac{C_p(T)}{T} dT = S(T)/N \\ k_B \log(\rho_N^v(E_N^*)) = N \cdot s(\varepsilon) \end{array} \right.$$



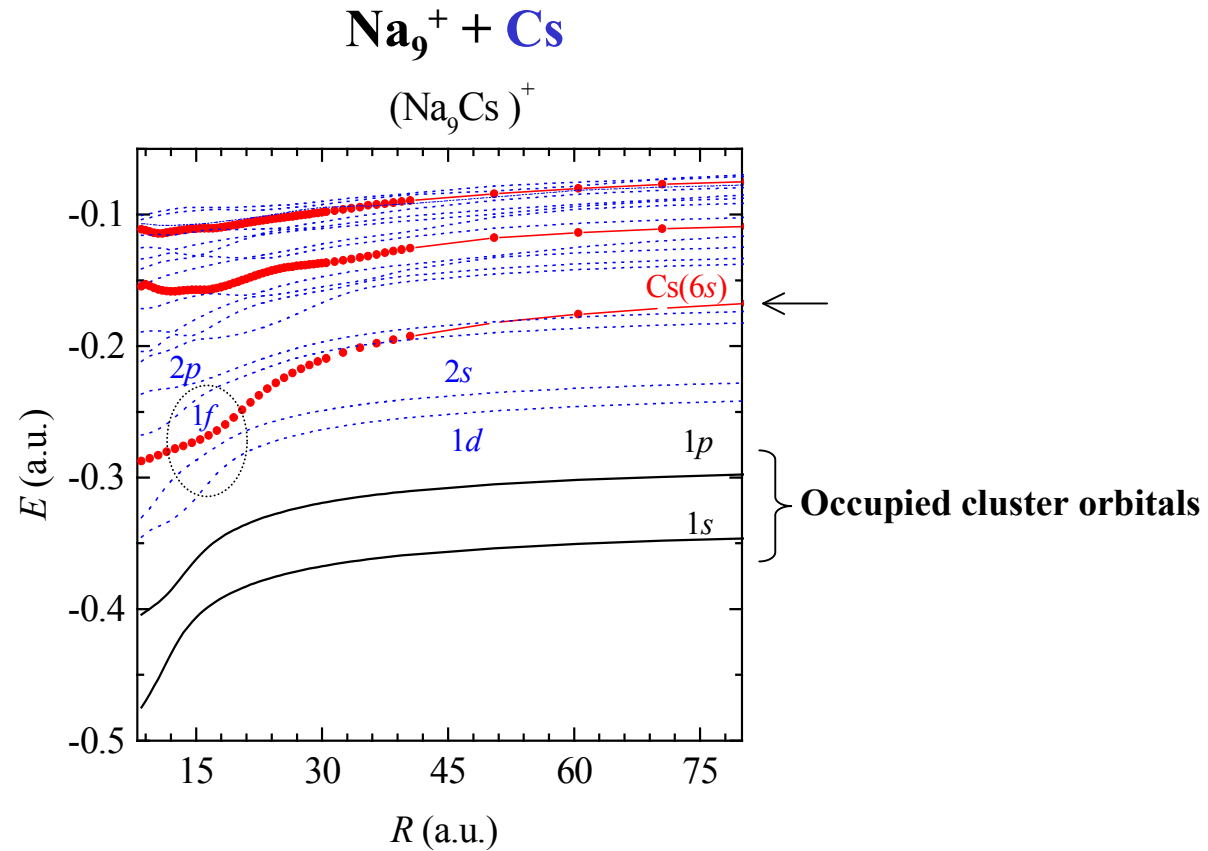
For one monomer



$$\frac{dN_{if}}{dt} \equiv k_{N,1}(E_N^*) = \frac{g^{(1)} \mu_1}{\hbar^3 \pi^2} \int_0^{E_N^* - D_{N,1}} \frac{\rho_{N-1}^v(E_N^* - D_{N,1} - e)}{\rho_N^v(E_N^*)} \sigma(e) e de$$

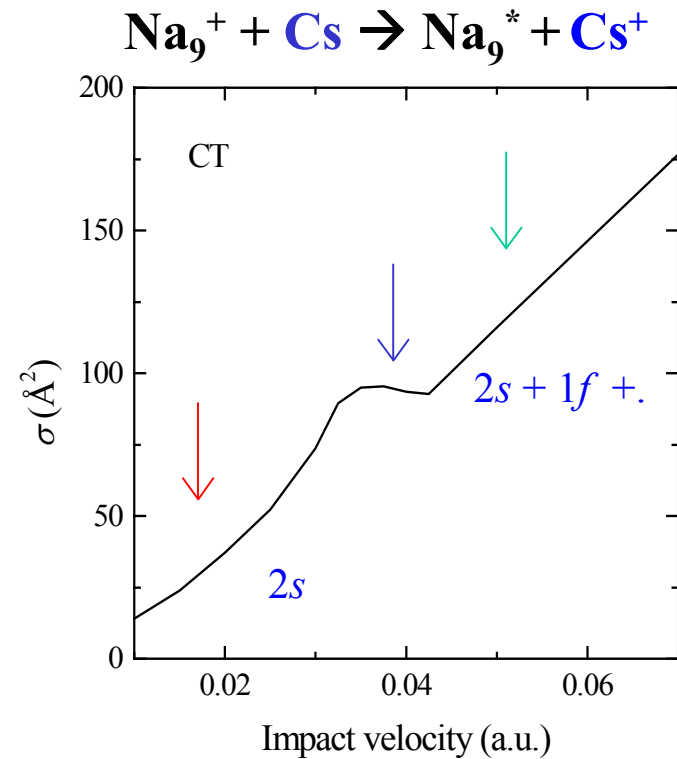
Coll. Spiegelman and Calvo-Lab. Physique Quantique-Toulouse

Correlation Diagram



- Capture *far away* from the cluster surface ($R_C = 8.3$ a.u.)
- Capture into *excited cluster orbitals* $1d$, $2s$, $1f$

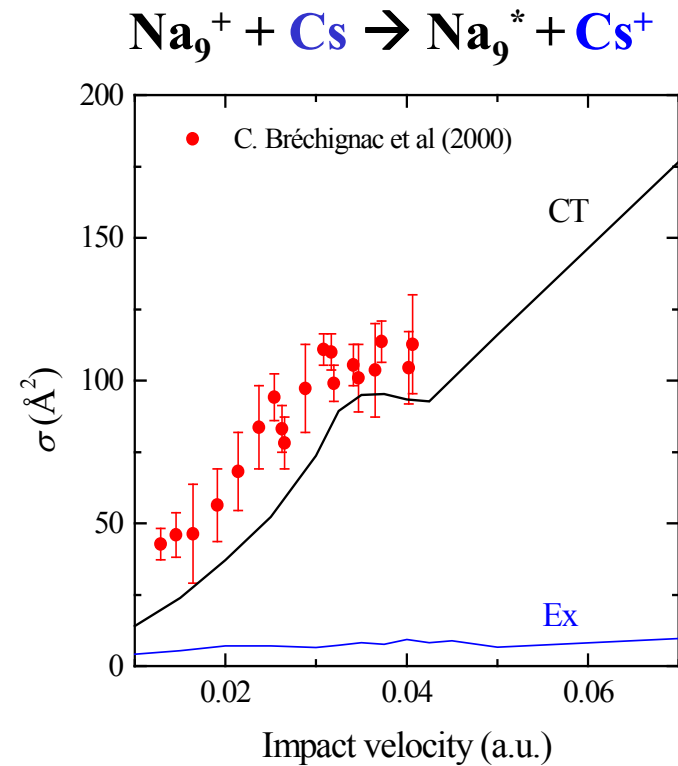
Charge Transfer Cross Section



B. Zarour et al.,
J. Phys. B 33, L707 (2000)

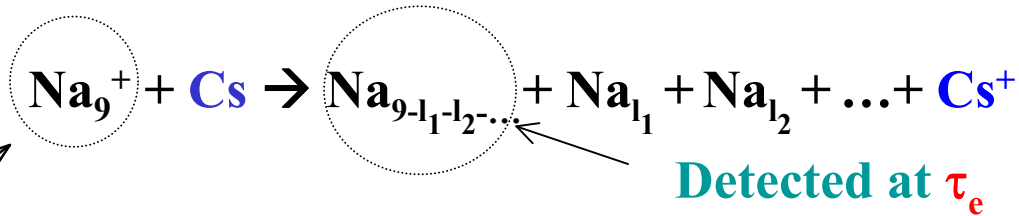
- Three regimes: rapid increase \rightarrow plateau \rightarrow rapid increase

Charge Transfer Cross Section

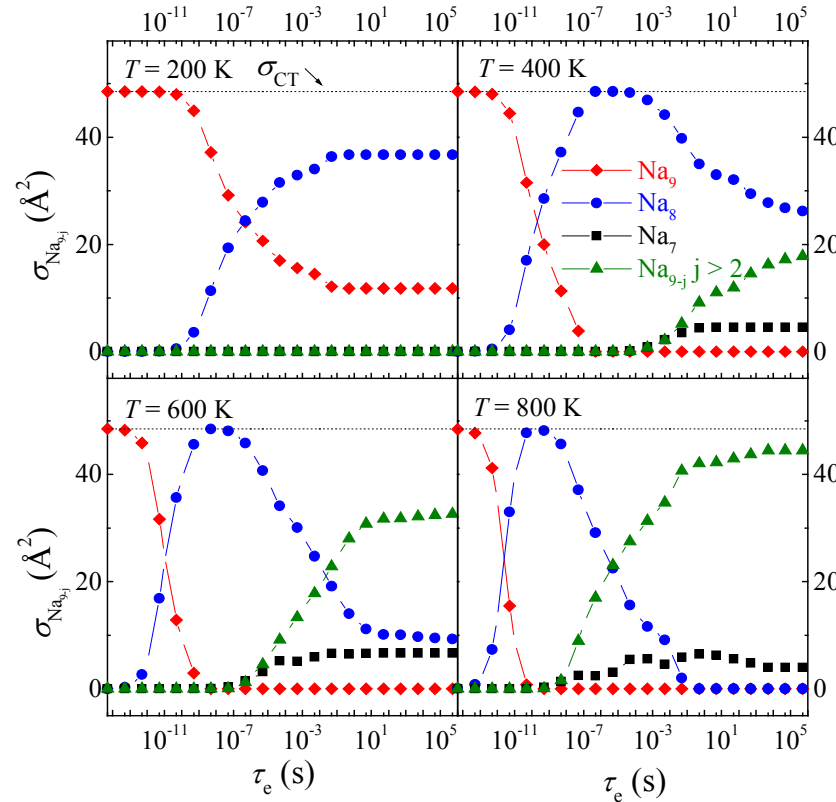


- **Excitation (Ex)** is much smaller than charge transfer (CT)
- CT is a **probe** of the cluster excited states

Charge Transfer Evaporation Cross Sections



Produced at T

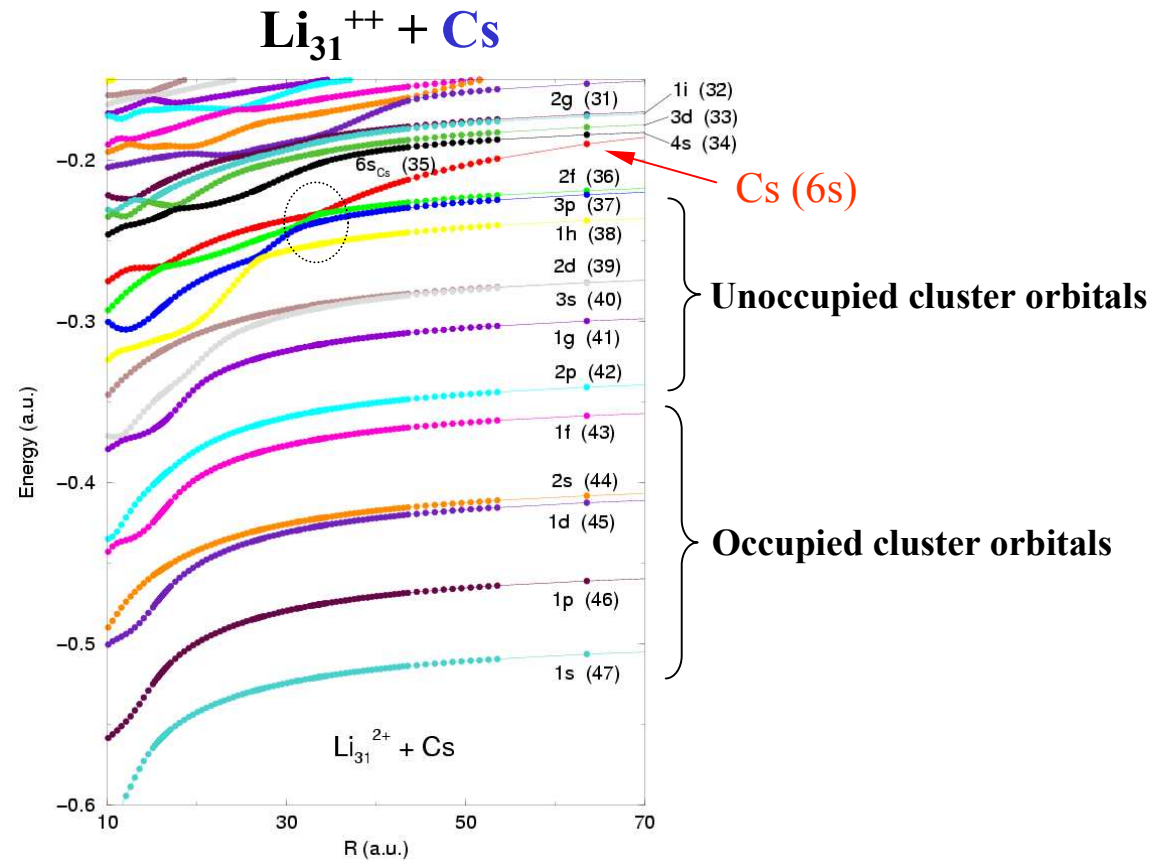


P. -A. Hervieux et al.,
J. Phys. B 34, 3331 (2001)

Fixed velocity
 $v_{\text{coll}} = 0.025 \text{ a.u.}$

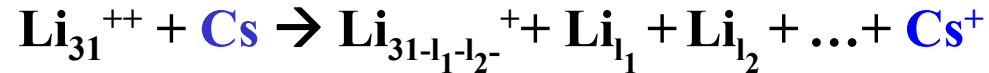
- The fragmentation cross sections **depend critically** on T and τ_e
- **Unfortunately** no absolute experimental measurements are available
detection of the neutrals !

Correlation Diagram



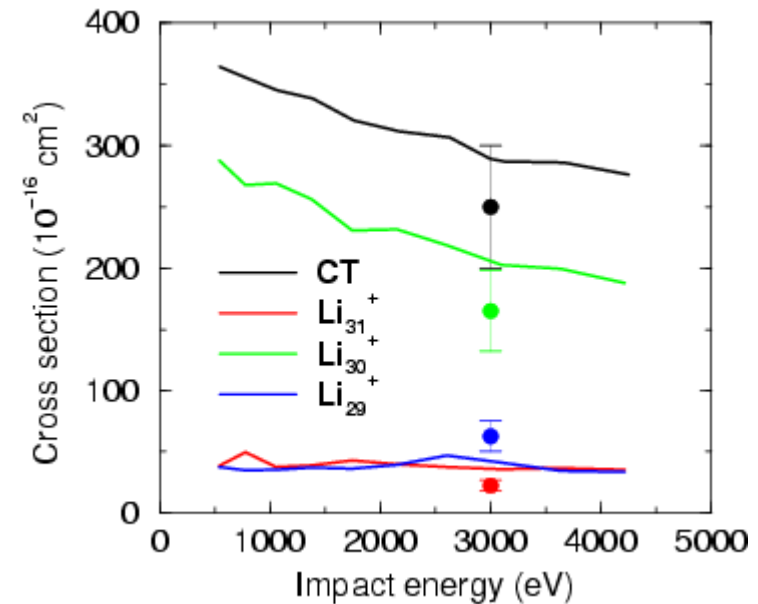
- Capture *far away* from the cluster surface ($R_C = 10.2 \text{ a.u.}$)

Charge Transfer Evaporation Cross Sections

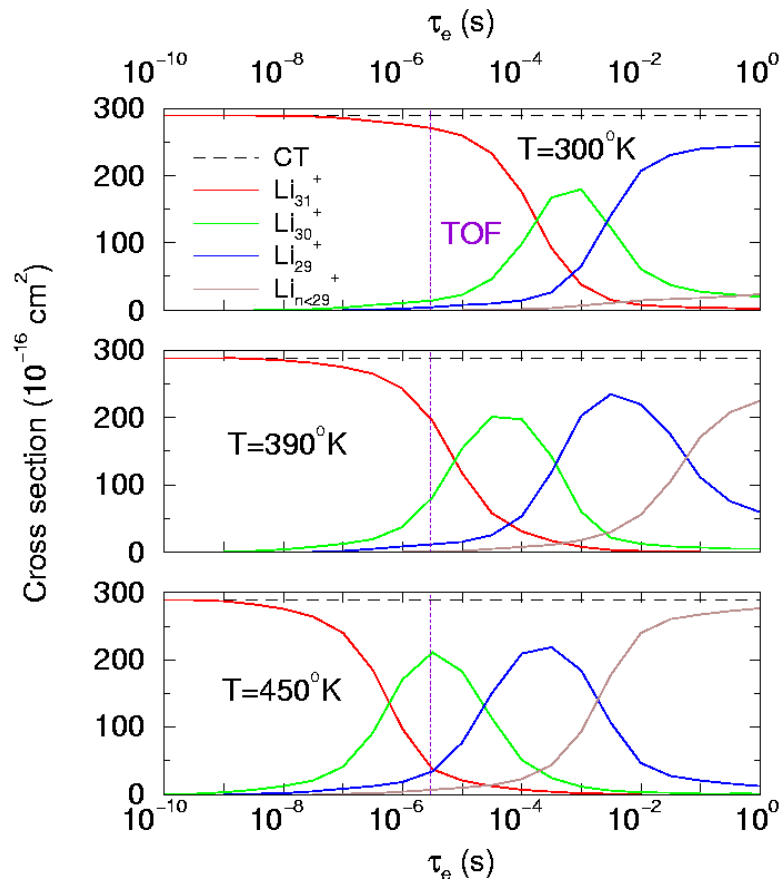
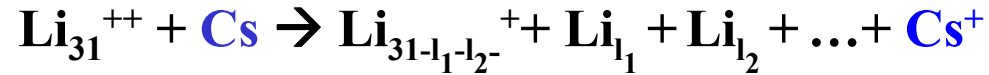


- Experiment: $420 < T < 660 \text{ K}$; $\tau_e = 3 \mu\text{s}$
- Theory: $T = 450 \text{ K}$; $\tau_e = 3 \mu\text{s}$

C. Bréchnac et al., Phys. Rev. Lett. **89**, 183402 (2002).
C. Bréchnac et al., Phys. Rev. A **68**, 063202 (2003).



Charge Transfer Evaporation Cross Sections



- **Good agreement Th/Ex** \rightarrow only possible with T and τ_e consistent with the experimental conditions

- **Small deviations from this choice** leads to **enormous differences** in the results

Fixed velocity

$E_{\text{coll}} = 3 \text{ keV}$

Conclusions (Metal Clusters)

- For CT good agreement with experimental measurements



validation of our Many-electron dynamical model

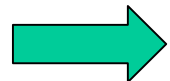
**DFT-LDAXC-SIC+Molecular Time-dependent close-coupling
+Inclusive probabilities**

- For CTE good agreement with experimental measurements



validation of our Fragmentation model

**Sequential evaporation of monomer or dimer + Microscopic Microcanonical
Statistical model of Weisskopf with bulk thermodynamical quantities +
experimental binding energies of the fragments**

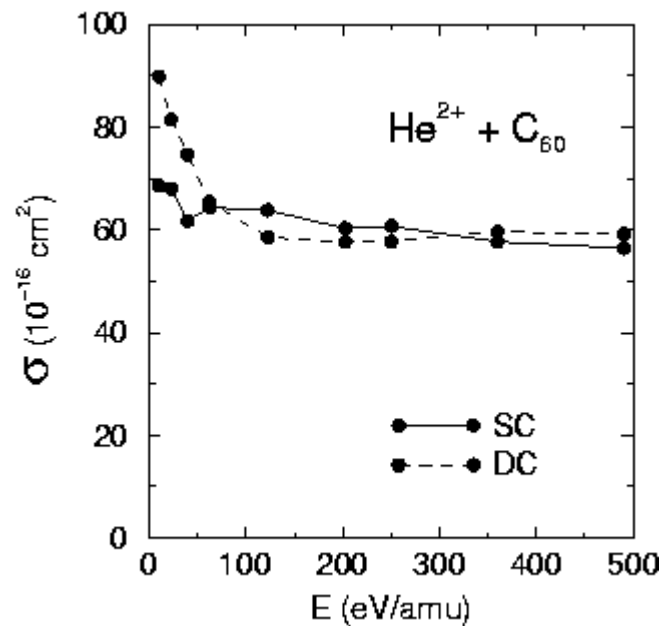
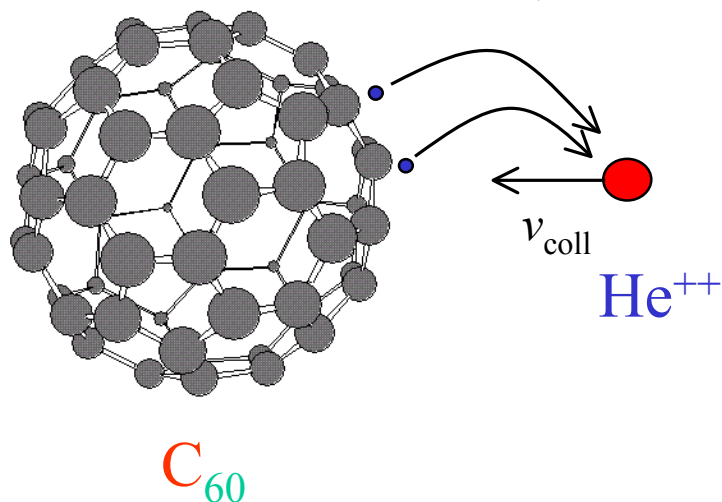


validation of our assumption of different time scales

Fullerenes

Charge Transfer Cross Section

L. F. Ruiz et al., *International Journal of Quantum Chemistry* **86**, 106 (2002).



- Same Theoretical Methods

- Single CT cross sections are comparable to double CT cross sections

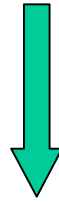
➡ Experimental measurements are available → P. Moretto-Capelle (Toulouse)

J. Phys. B **36**, 1585 (2003); *NIMB* **205**, 656 (2003).

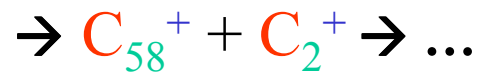
Charge Transfer Evaporation and Multifragmentation Cross Sections



Fast Process

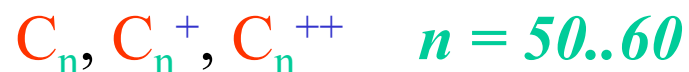


Slow Process



Charge Transfer Evaporation and Multifragmentation Cross Sections

- Real chemical bonds → With respect to metal clusters **much more complicated**
- Many isomers with *very different* dissociation energies
- DFT calculations of dissociation energies, ionization potential, entropy, geometries ...



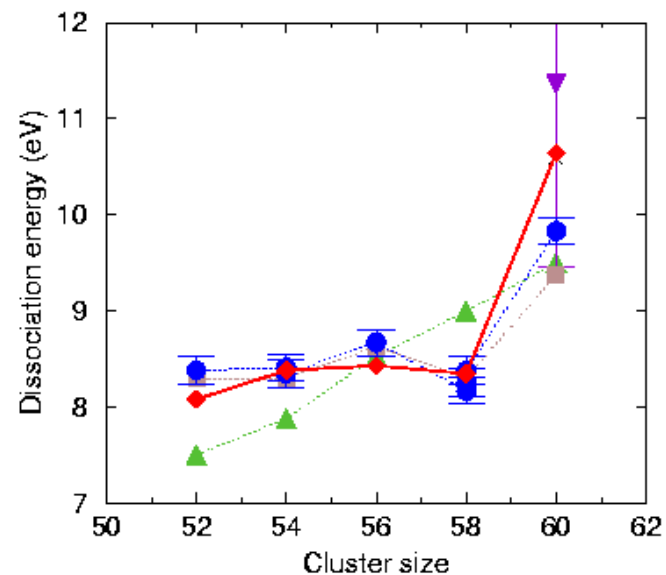
S. Diaz-Tendero et al., J. Chem. Phys. (2003).

Work in progress



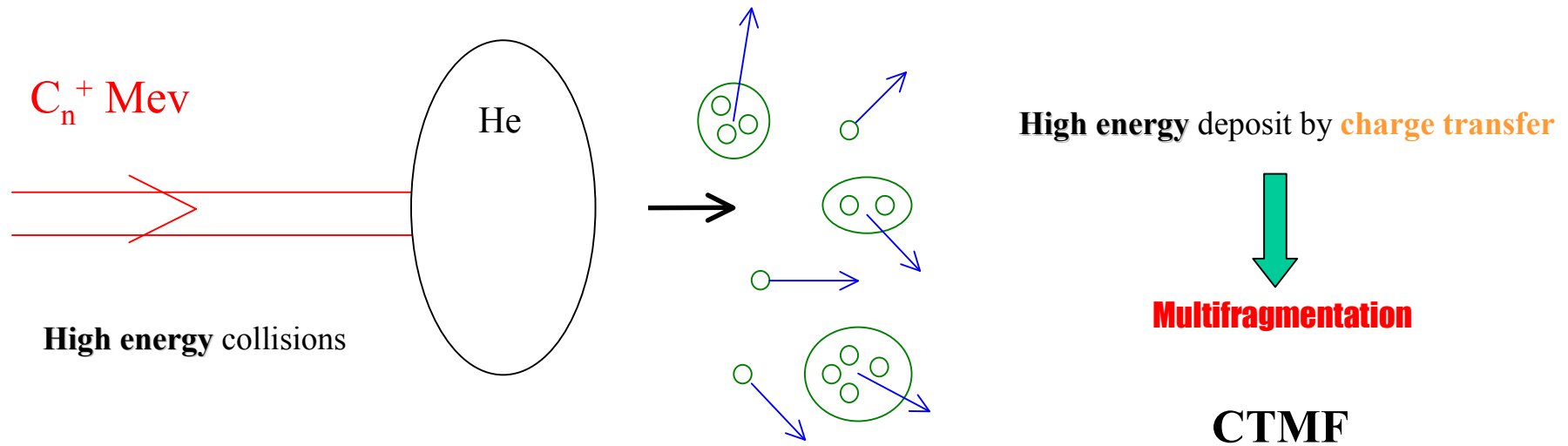
Sequential Evaporation of *dimers* → Weisskopf

Multifragmentation → MMMC



High Energy Fragmentation

Part II



Statistical Fragmentation of Small Neutral Carbon Clusters

CCSD(T)/6-311+G(3df)

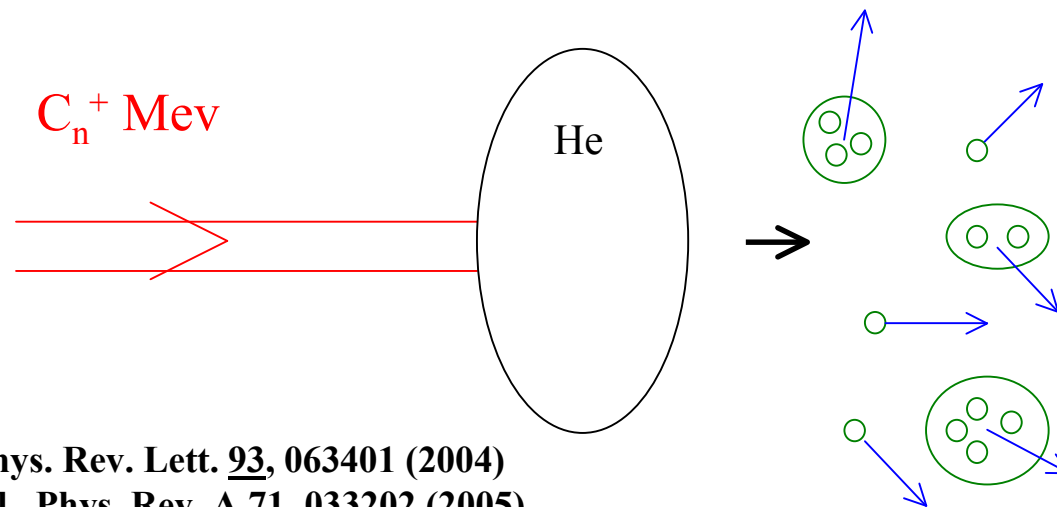
P. -A. Hervieux

IPCMS, University of Strasbourg

MMMC

S. Díaz-Tendero, F. Martín and M. Alcamí

Departamento de Química, University of Madrid, Spain



G. Martinet et al., Phys. Rev. Lett. 93, 063401 (2004)

S. Diaz-Tendero et al., Phys. Rev. A 71, 033202 (2005)

Microcanonical Metropolis Monte-Carlo (MMMC)

"Statistical Fragmentation of Hot Atomic Metal Clusters." D. H. E. Gross and P. -A. Hervieux, Z Phys. D 35, 27 (1995)

Problème:

Comment l'énergie d'excitation va-t-elle être distribuée parmi les différents degrés de liberté
Internes (vibrations), de translation de rotation ?

Taux de désintégration quantique (règle d'or de Fermi)

$$\frac{dN_{if}}{dt} = \frac{2\pi}{\hbar} |M_{if}|^2 \rho_f(E)$$

Hypothèse: $|M_{if}|^2 = cste$



Les transitions complexes sont contrôlées par *l'espace des phases accessible au système* avec les contraintes de conservation de:

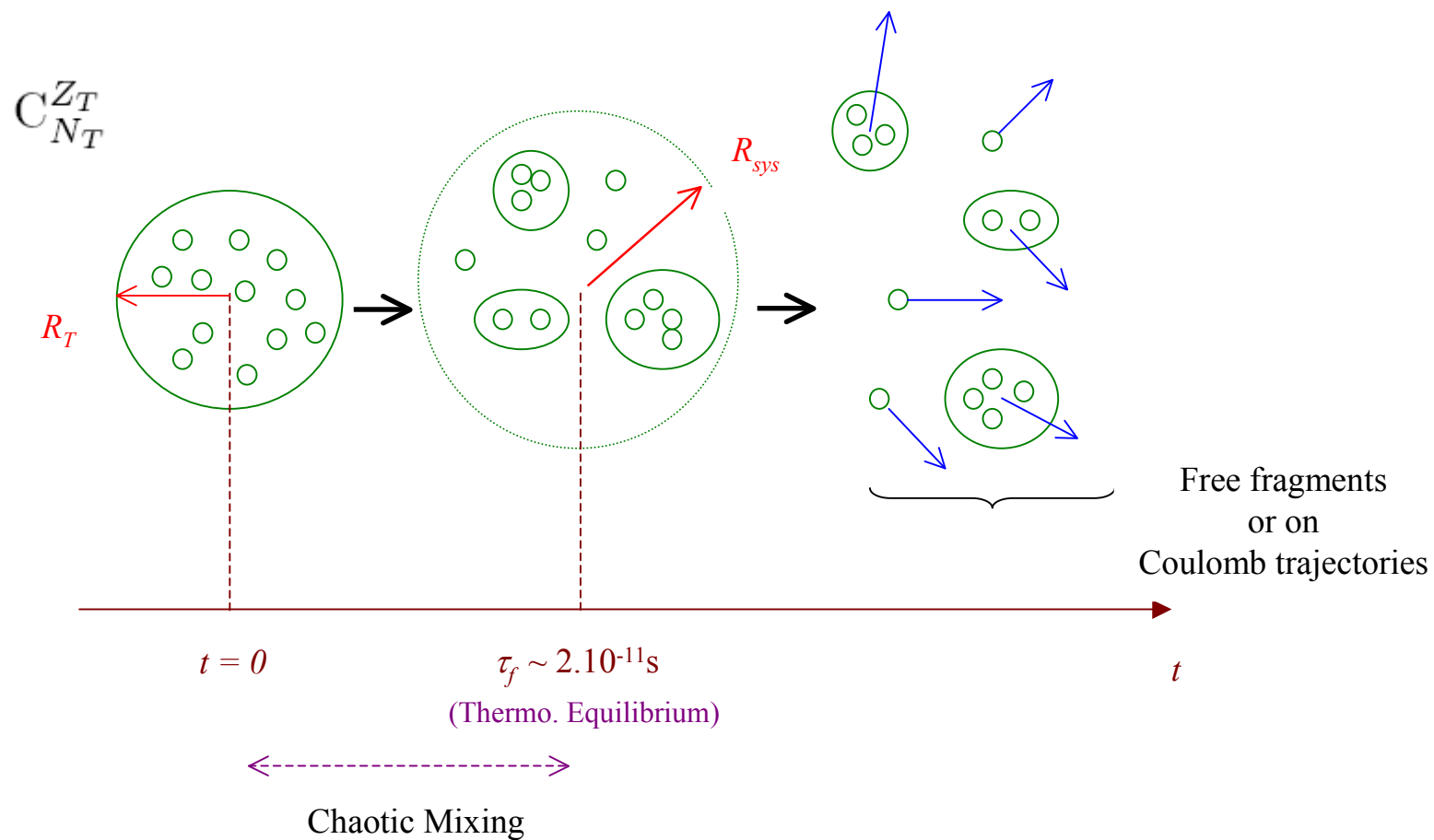
$$E_0, \mathbf{P}_0, \mathbf{L}_0, N_T, Z_T$$



Approche Statistique

Ensemble **microcanonique** → **essentiel** pour décrire correctement la thermodynamique des systèmes finis

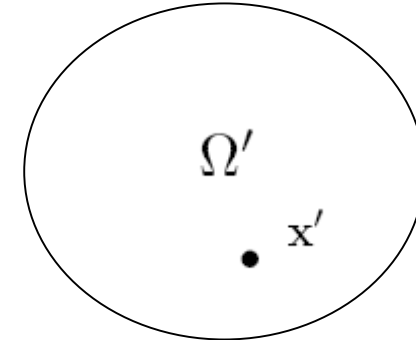
Microcanonical Metropolis Monte-Carlo



L'ensemble Microcanonique (définition)

Important car thermodynamique des systèmes finis !!!

$$\langle F \rangle = \frac{\int_{\Omega'} F(\mathbf{x}') w(\mathbf{x}') d\mathbf{x}'}{\int_{\Omega'} w(\mathbf{x}') d\mathbf{x}'}$$



- \mathbf{x}' est un point de l'espace des phases Ω'
- $Z = \int_{\Omega'} w(\mathbf{x}') d\mathbf{x}'$ est la fonction de partition
- $\frac{w(\mathbf{x}')}{\int_{\Omega'} w(\mathbf{x}') d\mathbf{x}'}$ est la fonction de distribution de l'ensemble microcanonique

$$\mathbf{x}' = \{N_f; \{N_j, Z_j, S_{ej}, O_{ej}, G_j\}_{j=1}^{N_f}; \{\mathbf{r}_j\}_{j=1}^{N_f}; \{\mathbf{P}_j\}_{j=1}^{N_f}; \{\phi_j\}_{j=1}^{N_f}; \{\mathbf{l}_j\}_{j=1}^{N_f}; \{E_{vj}^*\}_{j=1}^{N_f}\}$$

Spin électronique (pointing to S_{ej})
Géométrie (pointing to \mathbf{r}_j)
Moment orbital électronique (pointing to O_{ej})

Ensemble microcanonique $\Rightarrow E_0, \mathbf{P}_0, \mathbf{L}_0, N_T, Z_T$ fixés !

Poids microcanonique: $w(\mathbf{x}') d\mathbf{x}' = \delta(E - E_0) \delta(\mathbf{P} - \mathbf{P}_0) \delta(\mathbf{L} - \mathbf{L}_0) \delta(N - N_T) \delta(Z - Z_T) d\mathbf{x}'$

L'ensemble Microcanonique (conservations)

$$\mathbf{x}' = \{N_f; \{N_j, Z_j, S_{ej}, O_{ej}, G_j\}_{j=1}^{N_f}; \{\mathbf{r}_j\}_{j=1}^{N_f}; \{\mathbf{p}_j\}_{j=1}^{N_f}; \{\phi_j\}_{j=1}^{N_f}; \{\mathbf{l}_j\}_{j=1}^{N_f}; \{E_{vj}^*\}_{j=1}^{N_f}\}$$

Energie

$$E_0 = E_C + E_b + E_v^* + K_t + K_r;$$

$$E_C = \sum_{j < i} \frac{Z_i Z_j}{|\mathbf{r}_i - \mathbf{r}_j|};$$

$$E_b = \sum_{j=1}^{N_f} E_{bj};$$

$$E_v^* = \sum_{j=1}^{N_f} E_{vj}^*;$$

$$K_t = \sum_{j=1}^{N_f} \frac{\mathbf{p}_j^2}{2m_j};$$

$$K_r = \sum_{j=1}^{N_f} \left(\sum_{\nu=1}^{f_{rj}} \frac{\mathbf{l}_{\nu j}^2}{2I_{\nu j}} \right)$$

Impulsion

$$\mathbf{P} = \sum_j^{N_f} \mathbf{p}_j$$

Moment cinétique

$$\mathbf{L} = \sum_j \mathbf{l}_j + \sum_j (\mathbf{r}_j - \mathbf{R}_{cm}) \times (\mathbf{p}_j - \mathbf{P}_0).$$

Masse et Charge

$$\sum_{j=1}^{N_f} N_j = N_T$$

$$\sum_{j=1}^{N_f} Z_j = Z_T.$$

$$C_{N_T}^{Z_T}$$

Coll. P. Parneix and F. Calvo-Lab. PPM et Lab. Physique Quantique-Toulouse

L'ensemble Microcanonique (les poids statistiques)

$$\mathbf{x}' = \{N_f; \{N_j, Z_j, S_{ej}, O_{ej}, G_j\}_{j=1}^{N_f}; \{\mathbf{r}_j\}_{j=1}^{N_f}; \{\mathbf{P}_j\}_{j=1}^{N_f}; \{\phi_j\}_{j=1}^{N_f}; \{\mathbf{l}_j\}_{j=1}^{N_f}; \{E_{vj}^*\}_{j=1}^{N_f}\}$$

Poids microcanonique: $w(\mathbf{x}')d\mathbf{x}' = \delta(E - E_0)\delta(\mathbf{P} - \mathbf{P}_0)\delta(\mathbf{L} - \mathbf{L}_0)\delta(N - N_T)\delta(Z - Z_T)d\mathbf{x}'$

$$\langle F \rangle = \frac{\int_{\Omega'} F(\mathbf{x}')w(\mathbf{x}')d\mathbf{x}'}{\int_{\Omega'} w(\mathbf{x}')d\mathbf{x}'}$$

$$d\mathbf{x}' = \left(\prod_{j=1}^{N_f} \frac{d^3\mathbf{r}_j d^3\mathbf{p}_j}{(2\pi\hbar)^3} \right) \left(\prod_{j=1}^{N_f} \frac{d^{f_{rj}}\phi_j d^{f_{rj}}\mathbf{l}_j}{(2\pi\hbar)^{f_{rj}}\sigma_{rj}} \right) \times \left(\prod_{j=1}^{N_f} \rho_{vj}(E_{vj}^*)dE_{vj}^* \right)$$

\Rightarrow

$$\langle F \rangle = \frac{1}{Z} \sum_{N_f=1}^{N_T} w_{NZ}(N_f) \left[\sum_i^{N_{GS}} w_e(G_i, S_{ei}, O_{ei}) \times \int F(\mathbf{x}')\delta(E - E_0)\delta(\mathbf{P} - \mathbf{P}_0)\delta(\mathbf{L} - \mathbf{L}_0) \times \eta(\mathbf{r}_1, \mathbf{r}_2, \dots, \mathbf{r}_{N_f}) \prod_{j_i=1}^{N_f} \frac{d^3\mathbf{r}_{j_i} d^3\mathbf{p}_{j_i}}{(2\pi\hbar)^3} \times \prod_{j_i=1}^{N_f} \frac{d^{f_{rj_i}}\phi_{j_i} d^{f_{rj_i}}\mathbf{l}_{j_i}}{(2\pi\hbar)^{f_{rj_i}}\sigma_{rj_i}} \prod_{j_i=1}^{N_f} \rho_{vj_i}(E_{j_i}^*)dE_{vj_i}^* \right]$$

- f_{rj} : nombre de degrés de liberté de **rotation** du fragment j
- σ_{rj} : nombre de **symétrie** du fragment j
- ρ_{vj} : densité de niveaux **vibrationnels** du fragment j

L'ensemble Microcanonique (les poids)

Chaque configuration (\mathbf{x}_n) est associée à un **poids (entropie)**

$$w = \sum_{N_f=1}^{N_T} w_{NZ}(N_f) \sum_i w_{e_i} w_{\phi_i} w_{r_i} w_{q_i} w_{pl_i}$$

$$w_{NZ}(N_f) = \frac{1}{N_f!} \binom{N_T - 1}{N_f - 1} \binom{Z_T + N_f - 1}{N_f - 1}$$

$$w_e(G_i, S_{ei}, \mathcal{O}_{ei}) = \prod_{j=1}^{N_f} (2S_{ej} + 1) \mathcal{O}_{ej}$$

$$w_\phi = \prod_{j=1}^{N_l} \int \frac{d^2\phi_j}{(2\pi\hbar)^2 \sigma_{rj}} \prod_{i=1}^{N_c} \int \frac{d^3\phi_i}{(2\pi\hbar)^3 \sigma_{ri}}$$

$$w_r = \prod_{j=1}^{N_f} \int_{V_j} \eta(\mathbf{r}_1, \mathbf{r}_2, \dots, \mathbf{r}_{N_f}) \frac{1}{(2\pi\hbar)^3} d^3\mathbf{r}_j$$

$$w_q = \prod_{j=1}^{N_f} \rho_{vj}(E_{vj}^*) dE_{vj}^* \quad \rho_{vj}(E_{vj}^*) = \frac{(E_{vj}^*)^{f_{vj}-1}}{\Gamma(f_{vj}) \prod_{i=1}^{f_{vj}} (\hbar\nu_{ij})}$$

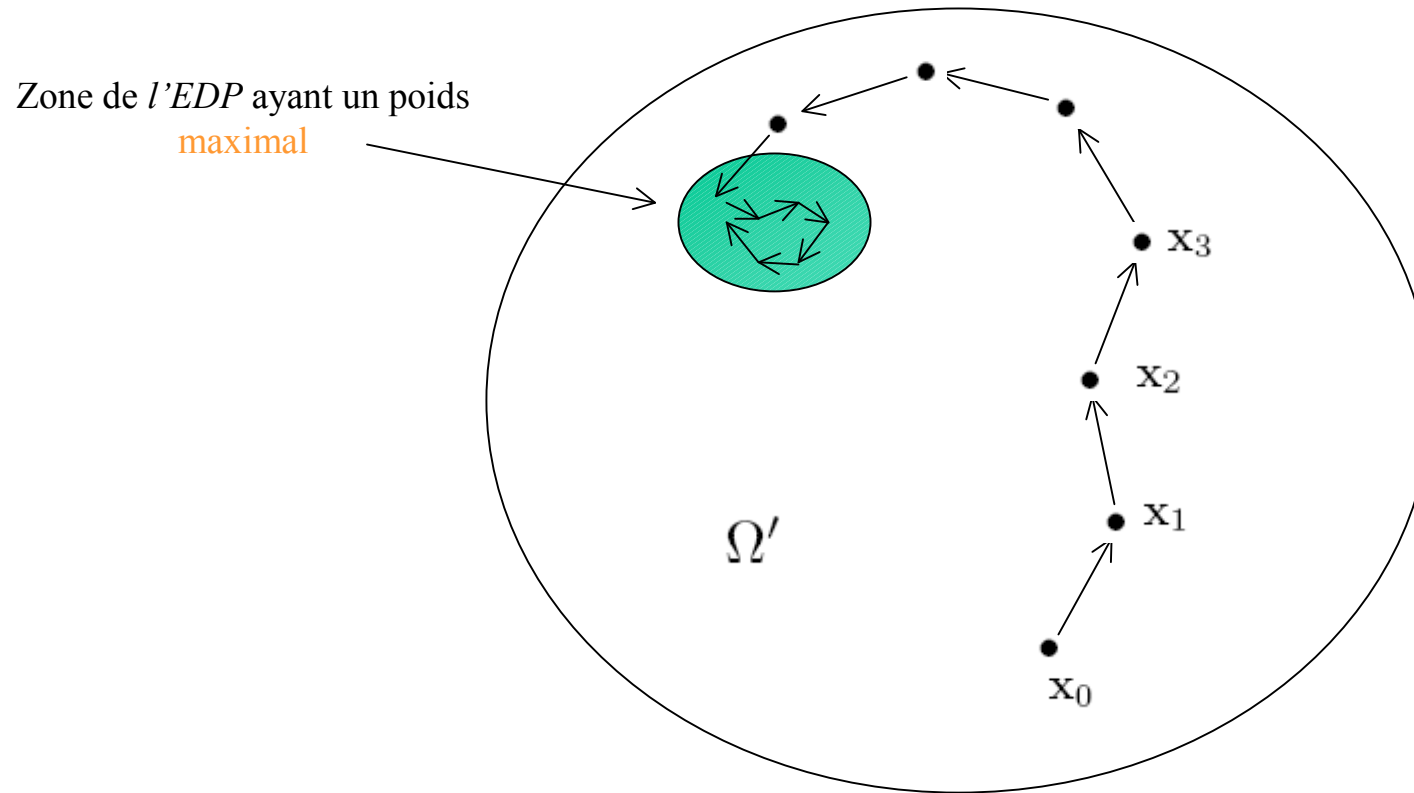
$$w_{pl} = \int \prod_{j=1}^{N_f} d^{f_{vj}} l_j \prod_{j=1}^{N_f} d^3 \mathbf{p}_j \delta(\mathbf{L} - \mathbf{L}_0) \delta(\mathbf{P} - \mathbf{P}_0) \delta(E - E_0)$$

harmonique

Les plus importants !

Méthode de Metropolis (1)

L'entropie d'un système fermé en équilibre statistique complet a la plus grande valeur possible



$\{x_0, x_1, \dots, x_n, x_{n+1} \dots\}$: chaîne de Markov

Comment génère t-on les points x_n ?

→ Importance Sampling, Méthode de Metropolis

Méthode de Metropolis (2-MC)

But: Trouver et explorer la partie de *l'espace des phases* qui contribue le plus à $\langle F \rangle$

1. On commence par générer un élément de Ω' de façon aléatoire $\mathbf{x}_0 \rightarrow w(\mathbf{x}_0) \equiv w_{old}$
2. On répète la même procédure $\mathbf{x}_1 \rightarrow w(\mathbf{x}_1) \equiv w_{new}$
3. On calcule $w_r = \frac{w_{new}}{w_{old}}$
4. Le nouvel état est accepté avec une probabilité w_r sinon \mathbf{x}_0 est enregistré avant de continuer.
5. Après on explore $\langle F \rangle = \frac{1}{N} \sum_{n=1}^N F(\mathbf{x}_n)$
 - Quand on passe de \mathbf{x}_n à \mathbf{x}_{n+1} peu de degrés de liberté doivent être changés
 - Les \mathbf{x}_n sont générés avec la probabilité $w(\mathbf{x}_n)/\mathcal{Z}$
 - N est de l'ordre de 10^7 événements

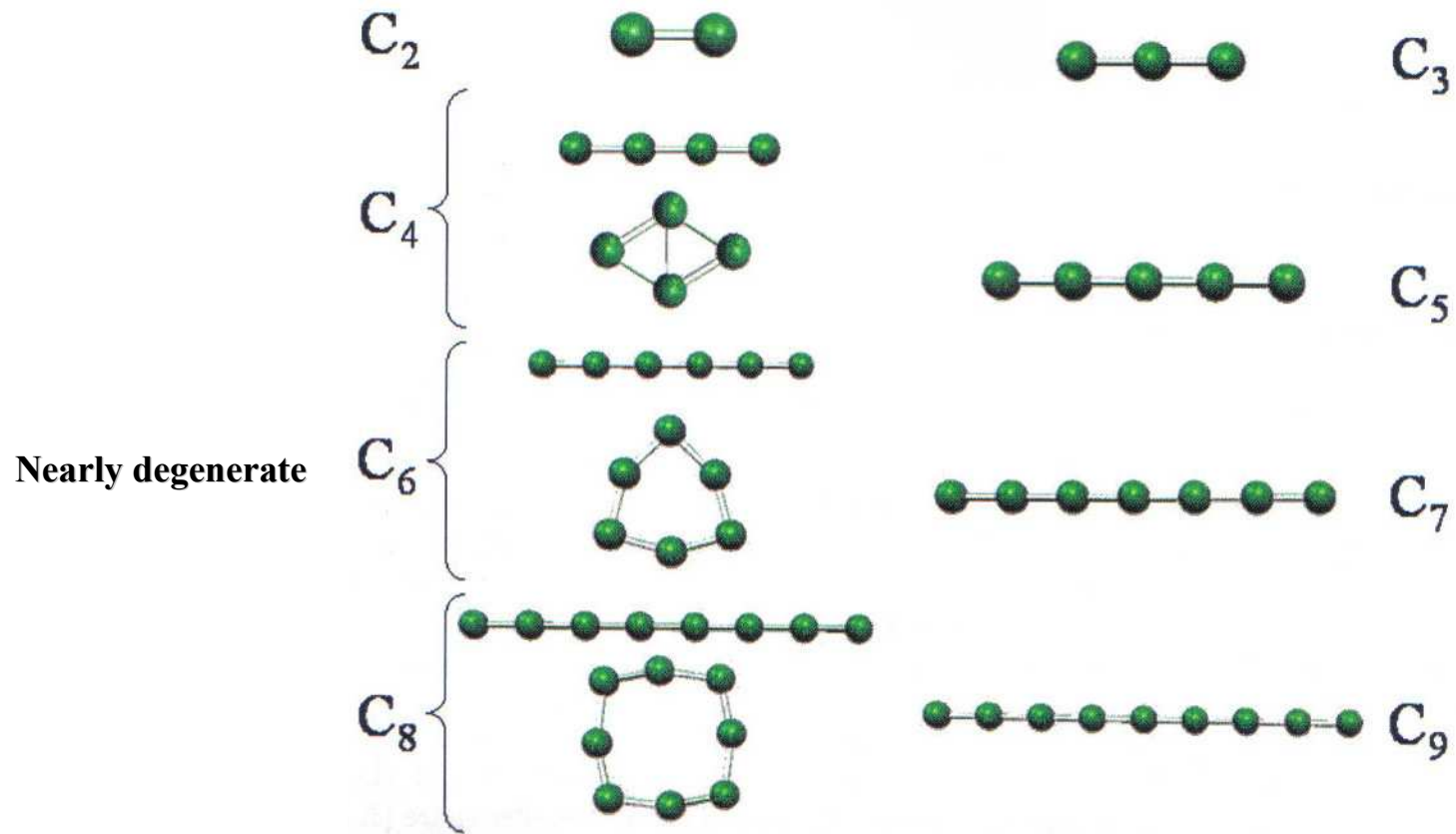
Monte-Carlo

$$\langle F \rangle = \frac{\int_{\Omega'} F(\mathbf{x}') w(\mathbf{x}') d\mathbf{x}'}{\int_{\Omega'} w(\mathbf{x}') d\mathbf{x}'}$$

CCSD(T)/6-311+G(3df) → Le coeur du MMC !

j	N	G	S_e	O_e	σ_r	$E + ZPE$ (au)	$\bar{\nu}$ (eV)	I_1/m_0 (Å ²)	I_2/m_0 (Å ²)	I_3/m_0 (Å ²)	R (Å)	D (eV) (l, k)	$\ln(\rho)$
1	1	A	1	5	0	-37.72589	0.000000	0.0000	0.0000	0.0000	0.76720	0.00000	0.00000
2	1	A	3	3	0	-37.77917	0.000000	0.0000	0.0000	0.0000	0.76720	0.00000	0.00000
3	2	L(D _{∞h})	1	1	2	-75.77837	0.232200	2.7764	2.7764	0.0000	0.62350	5.98737 (2,2)	3.24981
4	2	L(D _{∞h})	3	2	2	-75.75791	0.209800	3.0233	3.0233	0.0000	0.65050	5.43062 (2,2)	3.25365
5	3	L(D _{∞h})	1	1	2	-113.82422	0.049062	11.8262	11.8262	0.0000	1.28700	7.25679 (2,3)	19.29329
6	3	L(D _{∞h})	3	2	2	-113.74810	0.047823	11.8891	11.8891	0.0000	1.29000	5.18544 (2,3)	18.05127
7	3	C(C _{2v})	1	1	2	-113.78543	0.176400	2.8124	4.1746	6.9870	0.88300	6.20125 (2,3)	10.67926
8	3	C(D _{3h})	3	1	6	-113.79267	0.161110	3.3192	3.3192	6.6384	0.78700	6.39826 (2,3)	11.04509
9	4	L(D _{∞h})	1	1	2	-151.76200	0.067399	30.1371	30.1371	0.0000	1.95050	4.31603 (2,5)	24.32874
10	4	L(D _{∞h})	3	1	2	-151.73920	0.068026	30.0438	30.0438	0.0000	1.94950	3.69561 (2,5)	23.17758
11	4	C(D _{2h})	1	1	4	-151.78067	0.099871	3.9768	10.8631	14.8399	1.23300	4.82407 (2,5)	20.08692
12	4	C(D _{2h})	3	1	4	-151.74738	0.089866	4.4024	10.1261	14.5285	1.19100	3.91820 (2,5)	19.47235
13	5	L(D _{∞h})	1	1	2	-189.81595	0.066190	58.4789	58.4789	0.0000	2.56000	5.80587 (3,5)	34.13635
14	5	L(D _{∞h})	3	2	2	-189.73064	0.078498	58.3638	58.3638	0.0000	2.55000	3.48445 (3,5)	27.32531
15	5	C(C _s)	1	1	1	-189.64652	0.137100	8.3280	14.8329	22.9043	1.33200	1.19541 (3,5)	10.96461
16	5	C(C ₂)	3	1	1	-189.70491	0.093690	6.9822	17.7999	23.9031	1.45100	2.78429 (3,5)	22.00066
17	6	L(D _{∞h})	1	1	2	-227.77243	0.063565	103.1003	103.1003	0.0000	3.21550	3.37397 (5,5)	34.13085
18	6	L(D _{∞h})	3	1	2	-227.77657	0.064024	102.9515	102.9515	0.0000	3.21350	3.48662 (5,5)	34.46429
19	6	C(D _{3h})	1	1	6	-227.79560	0.111200	17.9057	17.9160	35.8216	1.46380	4.00446 (5,5)	27.90159
20	6	C(C _{2v})	3	1	2	-227.70536	0.098552	16.2726	21.4667	37.7393	1.56460	1.54888 (5,5)	17.95206
21	7	L(D _{∞h})	1	1	2	-265.80739	0.061928	162.9505	162.9501	0.0000	3.83300	5.51035 (5,11)	46.62335
22	7	L(D _{∞h})	3	2	2	-265.73061	0.058380	165.1399	165.1399	0.0000	3.85650	3.42104 (5,11)	39.94042
23	7	C(C _{2v})	1	1	2	-265.78847	0.090119	22.6989	33.2893	55.9883	1.67900	4.99551 (5,11)	37.67528
24	7	C(C _{2v})	3	1	2	-265.76765	0.077859	24.4609	33.4754	57.9363	1.71200	4.42896 (5,11)	38.06315
25	8	L(D _{∞h})	1	1	2	-303.80799	0.059952	245.5097	245.5097	0.0000	4.48450	4.56671 (5,13)	48.82201
26	8	L(D _{∞h})	3	1	2	-303.80774	0.060272	245.2952	245.2952	0.0000	4.48250	4.55992 (5,13)	48.69259
27	8	C(C _{4h})	1	1	8	-303.82401	0.084327	40.3222	40.3222	80.6444	1.83700	5.00256 (5,13)	42.82220
28	8	C(D _{4h})	3	1	8	-303.80000	0.077042	39.9843	40.0037	79.9880	1.83000	4.34923 (5,13)	41.92940
29	9	L(D _{∞h})	1	1	2	-341.84056	0.059335	348.2156	348.2156	0.0000	5.10648	6.00668 (5,19)	59.24780
30	9	L(D _{∞h})	3	1	2	-341.69013	0.054610	351.4200	351.4200	0.0000	5.13403	1.91333 (5,19)	35.90483
31	9	C(C _s)	3	1	1	-341.72629	0.069421	56.0323	57.1993	112.4990	2.03993	2.59147 (5,19)	36.67573
32	9	C(C _s)	3	3	1	-341.71505	0.073154	55.2419	58.2259	113.4680	2.04124	2.28561 (5,19)	32.93837

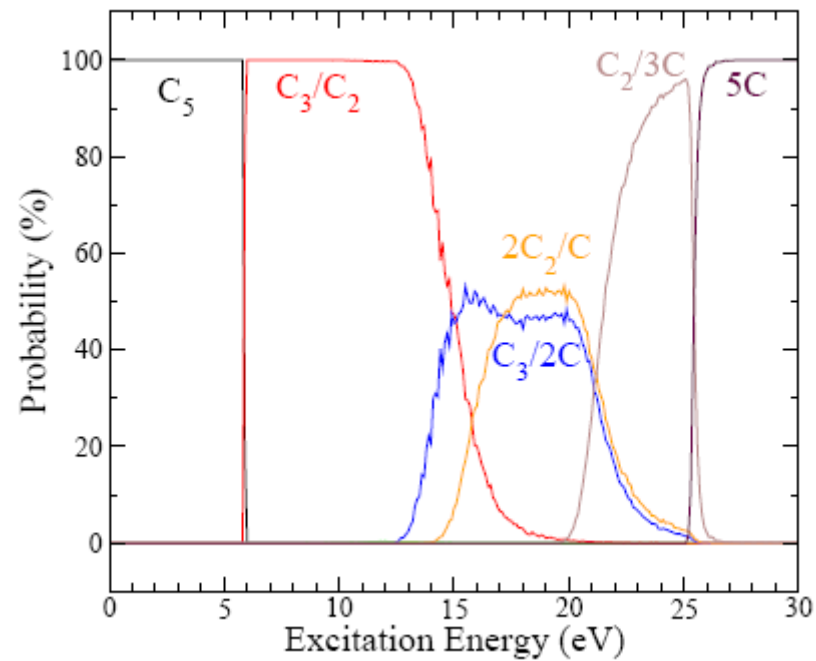
Most stable isomers B3LYP 6-311+G(3df)



MMMC C₅

7 fragmentation channels: C₅, C₄/C, C₃/C₂, C₃/C/C, C₂/C₂/C, C₂/C/C/C; C/C/C/C/C

Number of emitted fragments	Deexcitation channel
1	C ₅
2	C ₃ /C ₂
	C ₄ /C
3	C ₃ /C/C
	C ₂ /C ₂ /C
4	C ₂ /C/C/C
5	C/C/C/C/C

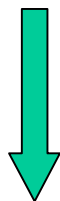


C₅ (isomer analysis)

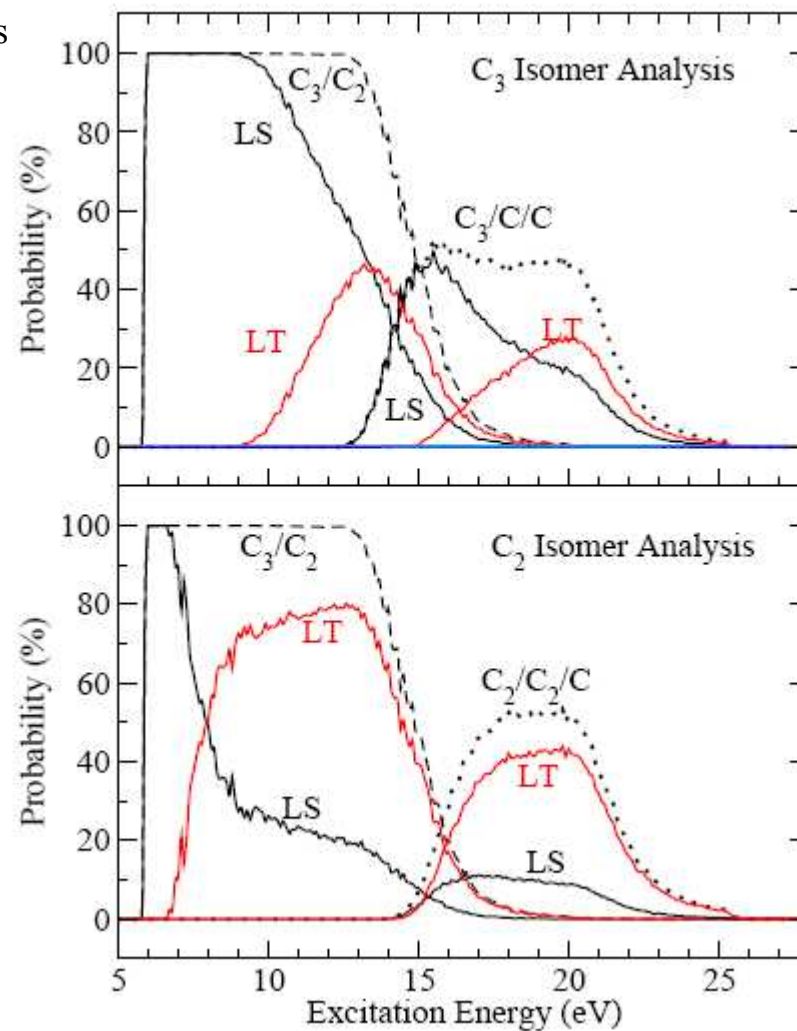
Isomer analysis of the C₃/C₂, C₃/C/C and C₂/C₂/C channels

LT: Linear Triplet
LS: Linear Singlet

- Cyclic isomeric forms of C₃ or C₂ are **never observed**
- Low energy: LS
- High energy: **LT**



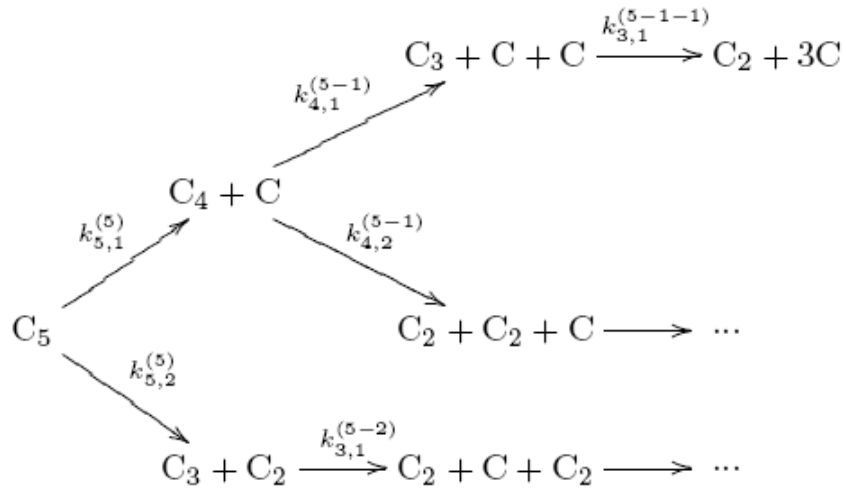
All isomeric forms must be included



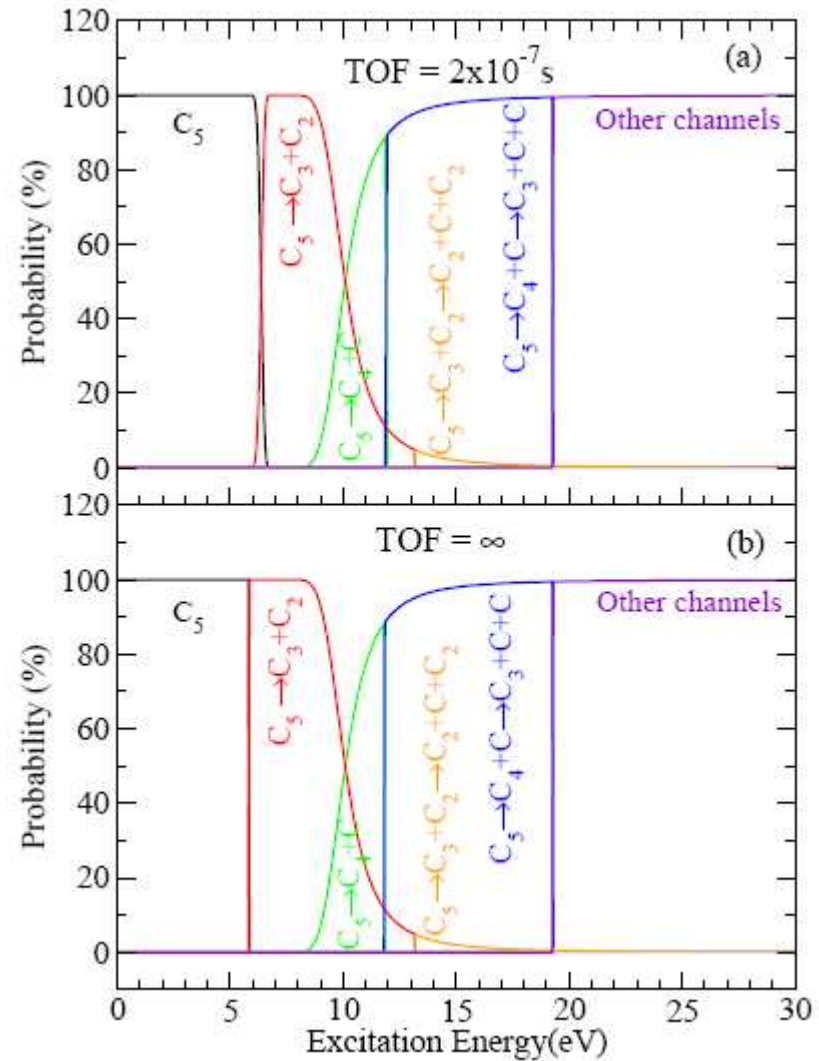
C₅

Time dependent Weisskopf calculations

Including **monomer**, **dimer** and **trimer** evaporation

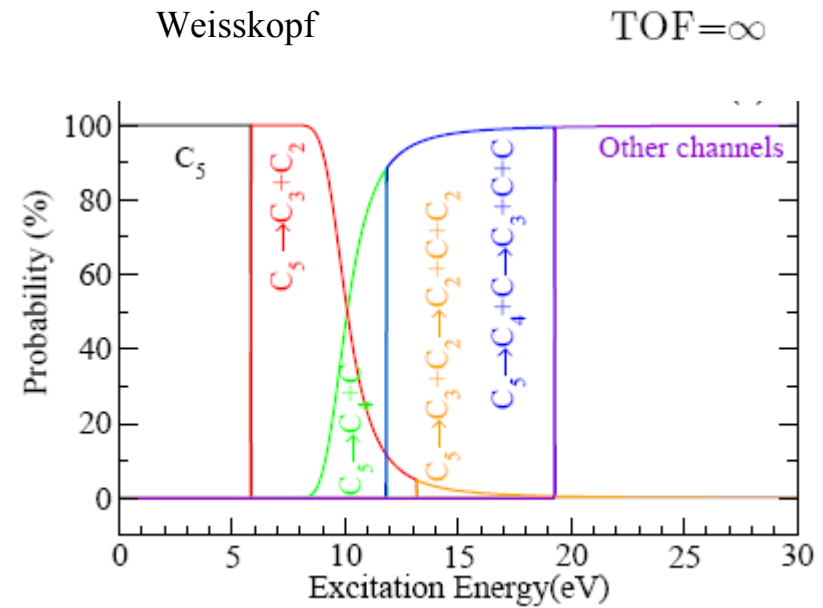
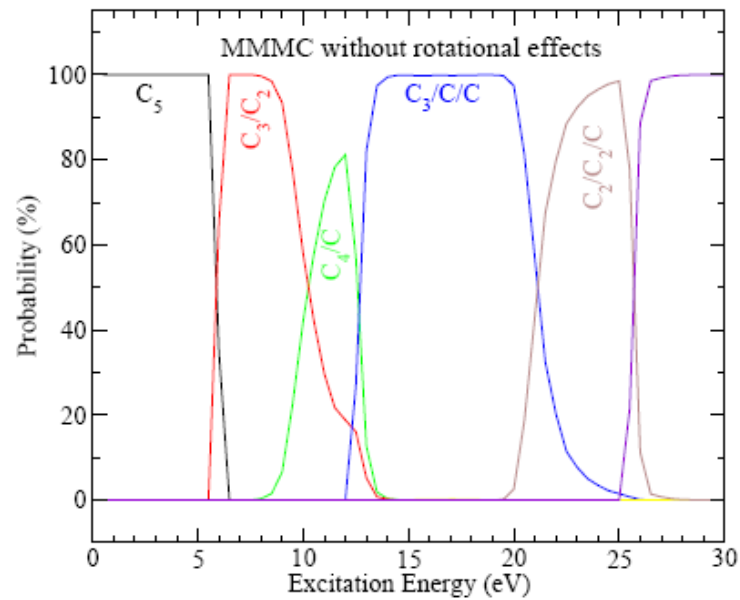


MMC is compatible with the experimental conditions



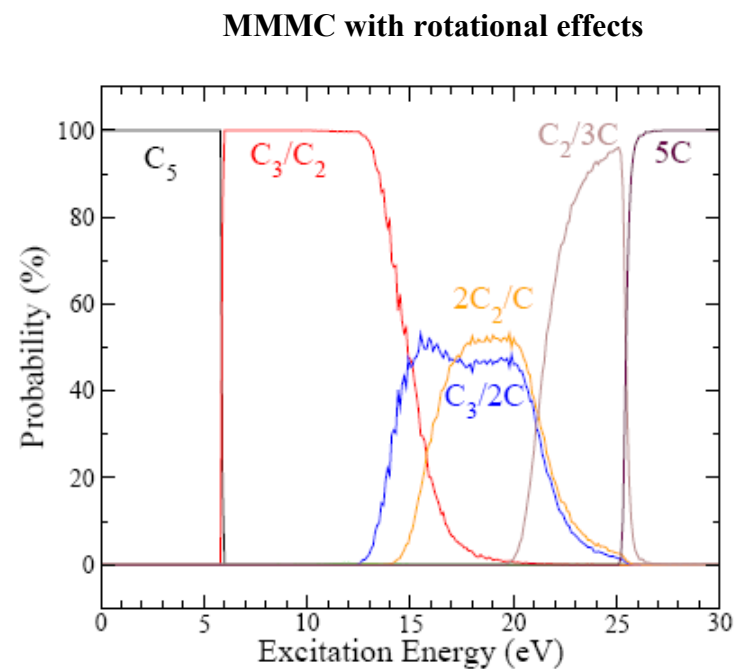
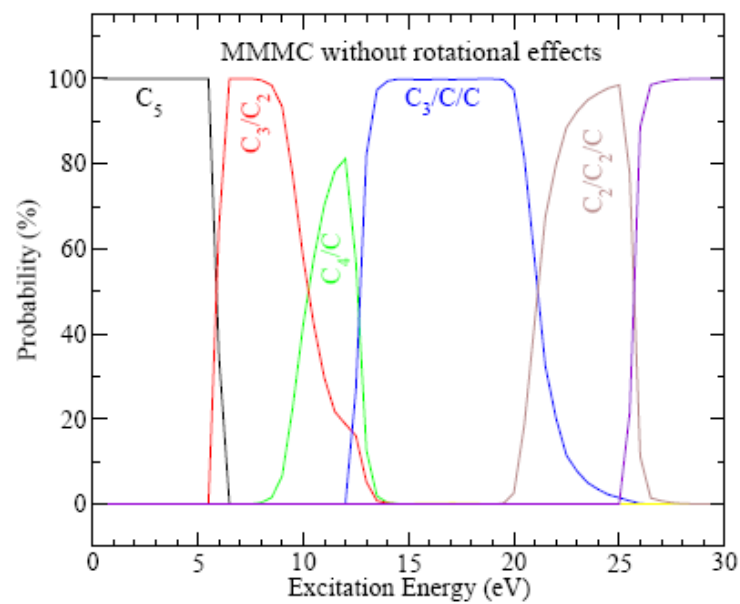
C₅

Equivalence between MMMC and Weisskopf



C₅

Rotational effects

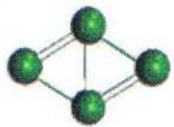
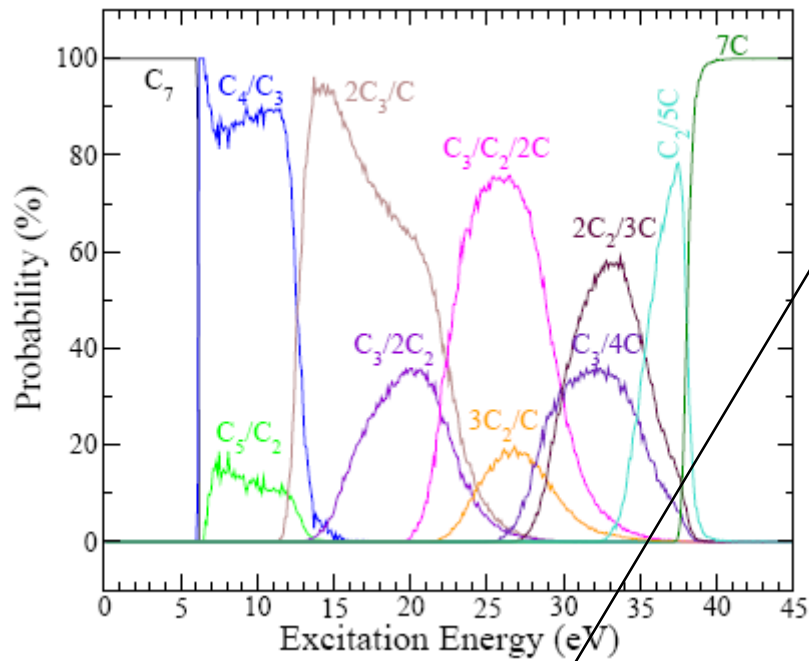


Rotational effects play a very important role in the fragmentation process !

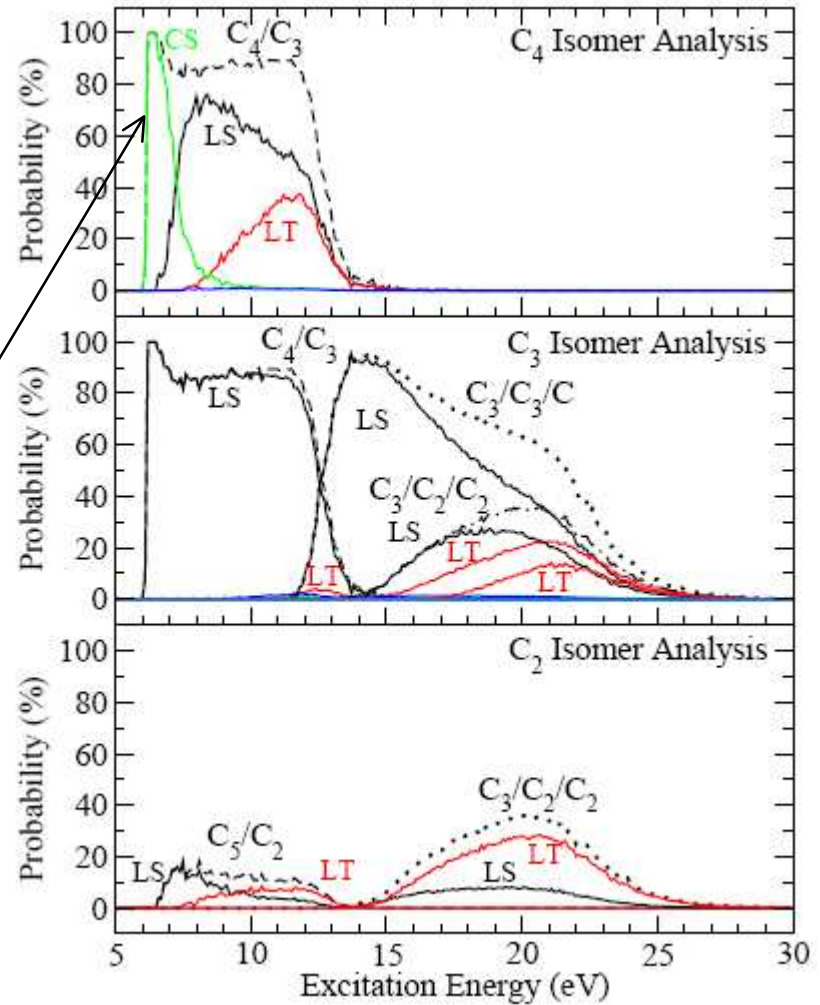
C₇

15 fragmentation channels

C₇, C₆/C, C₅/C₂, C₄/C₃, C₃/C₃/C, ...



CS: Cyclic Singlet

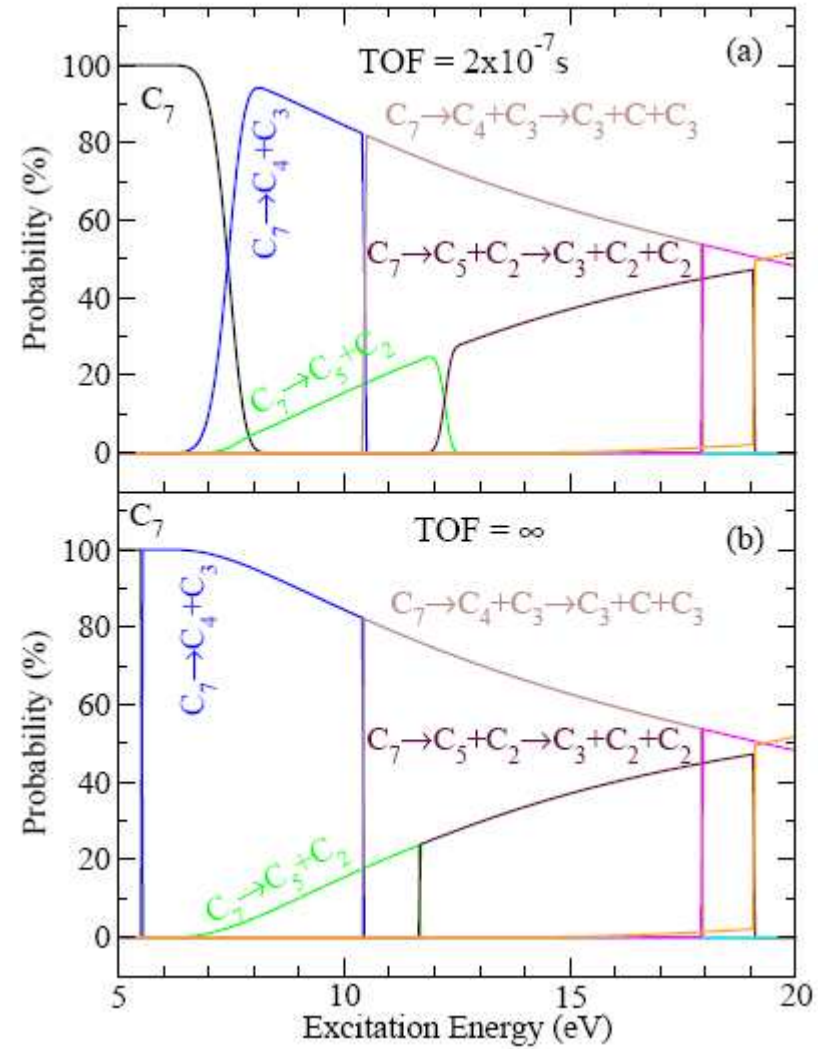


C₇

Time dependent Weisskopf calculations



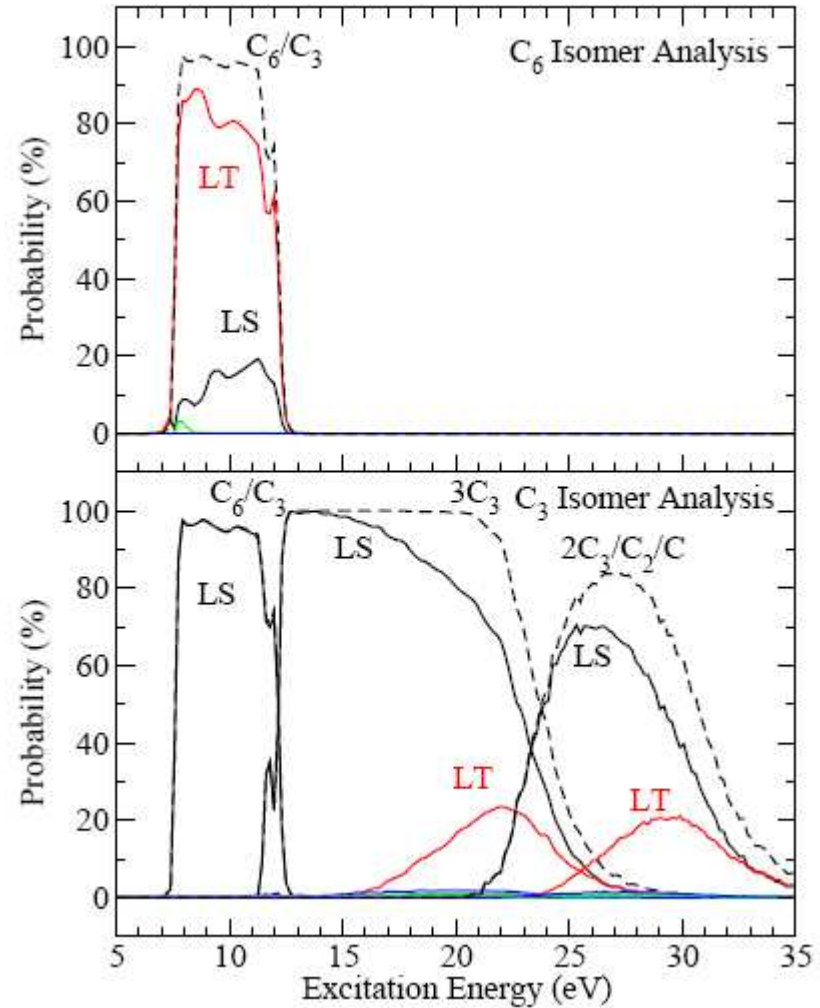
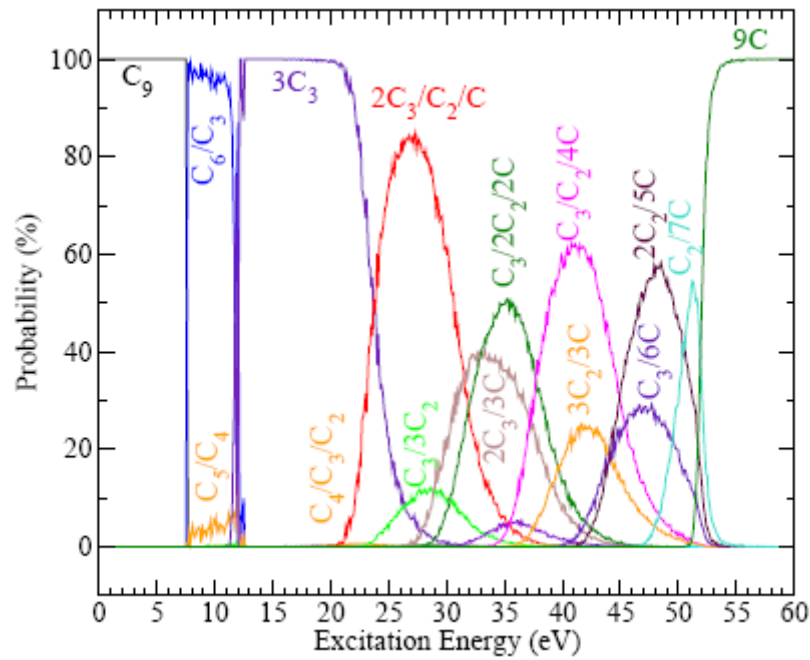
MMMC is compatible with the experimental conditions



C₉

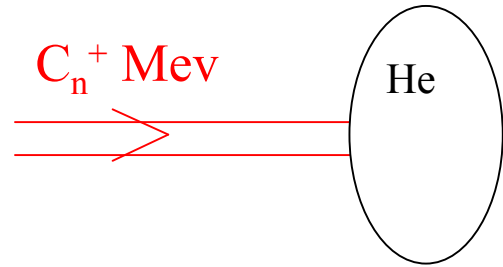
30 fragmentation channels

C₉, C₈/C, C₇/C₂, C₆/C₃, ...

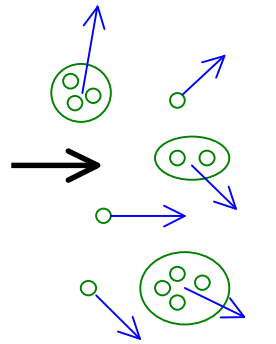


The formation of C₃(linear) play a dominant role !

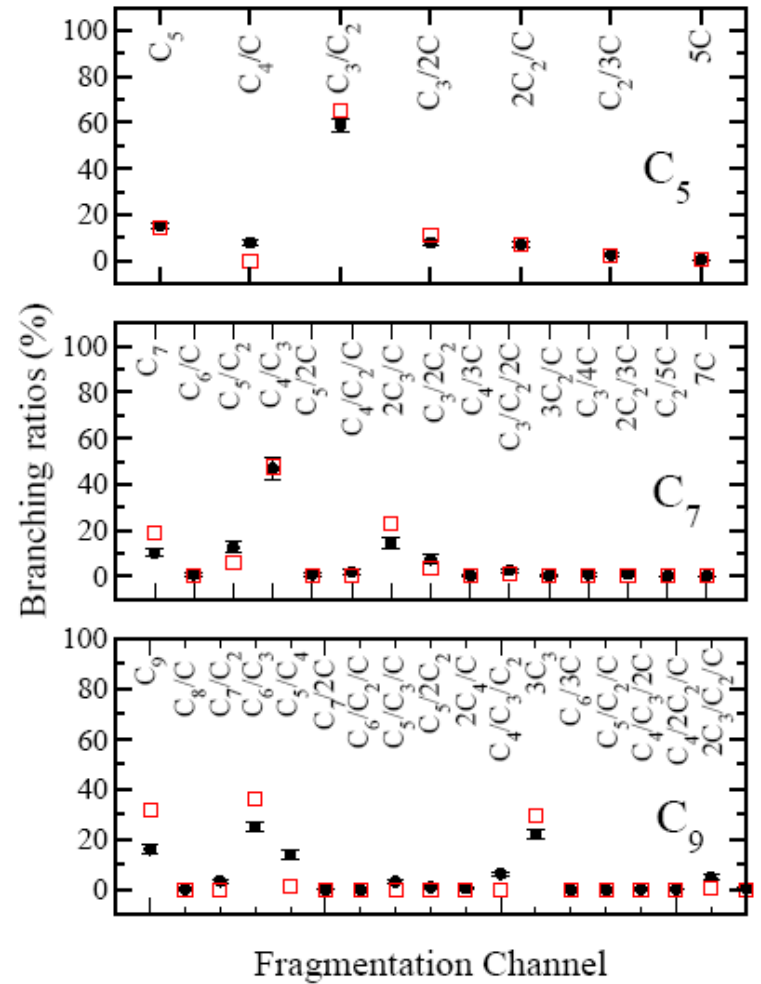
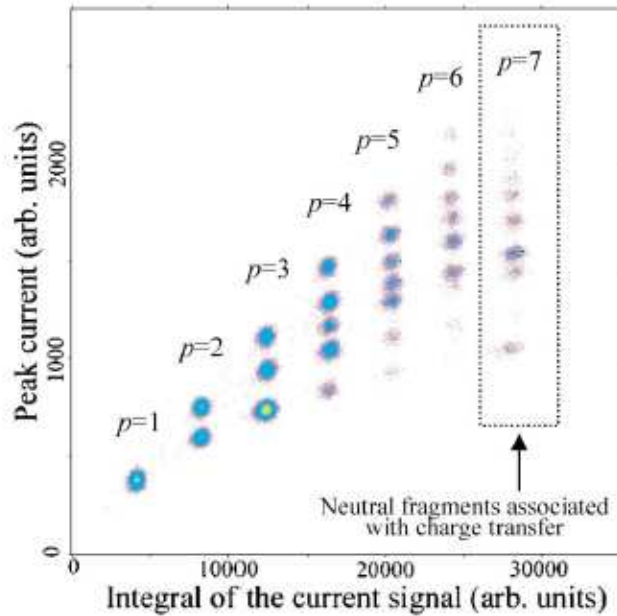
Theory/Experiment



IPN, Orsay
(K. Woehrer et M. Chabot)

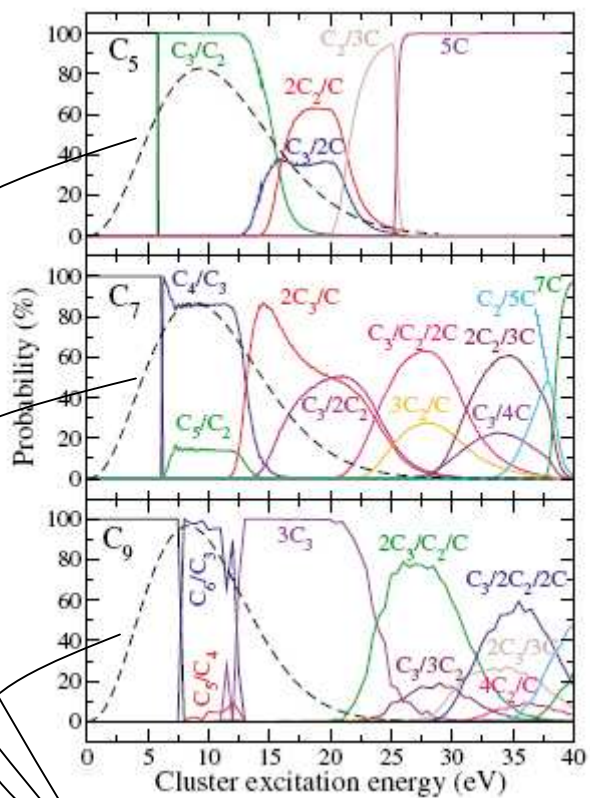


Neutral fragments



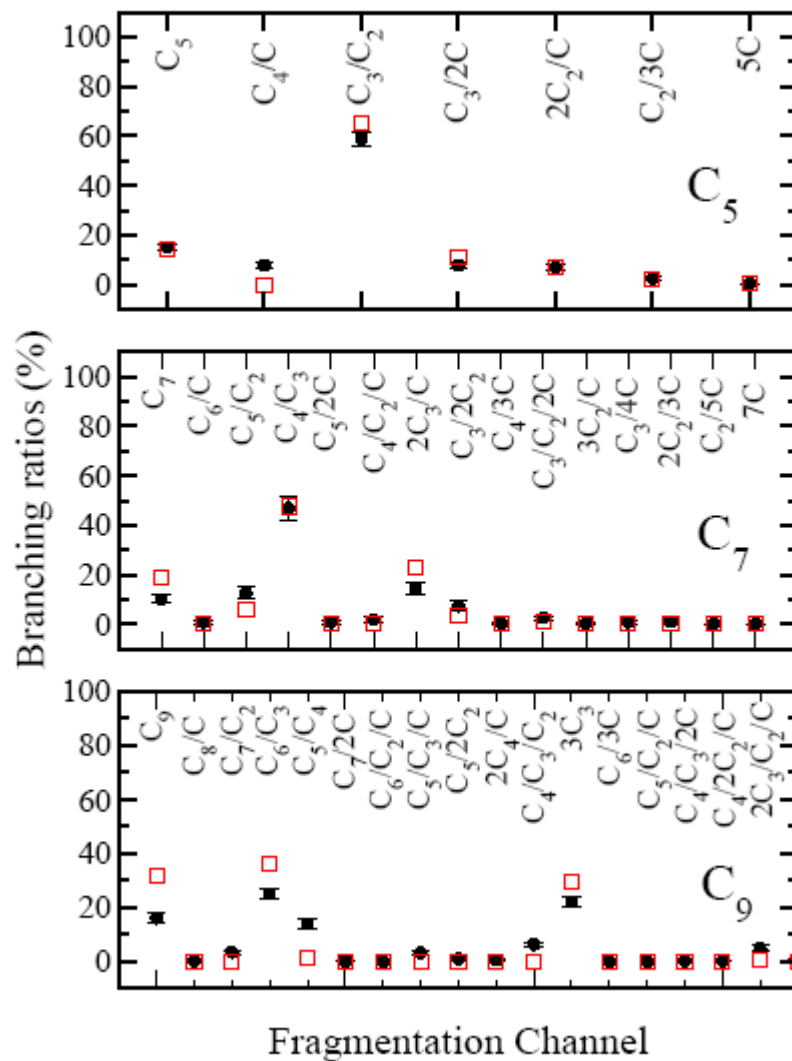
G. Martinet et al., Phys. Rev. Lett. 93, 063401 (2004)

Theory/Experiment

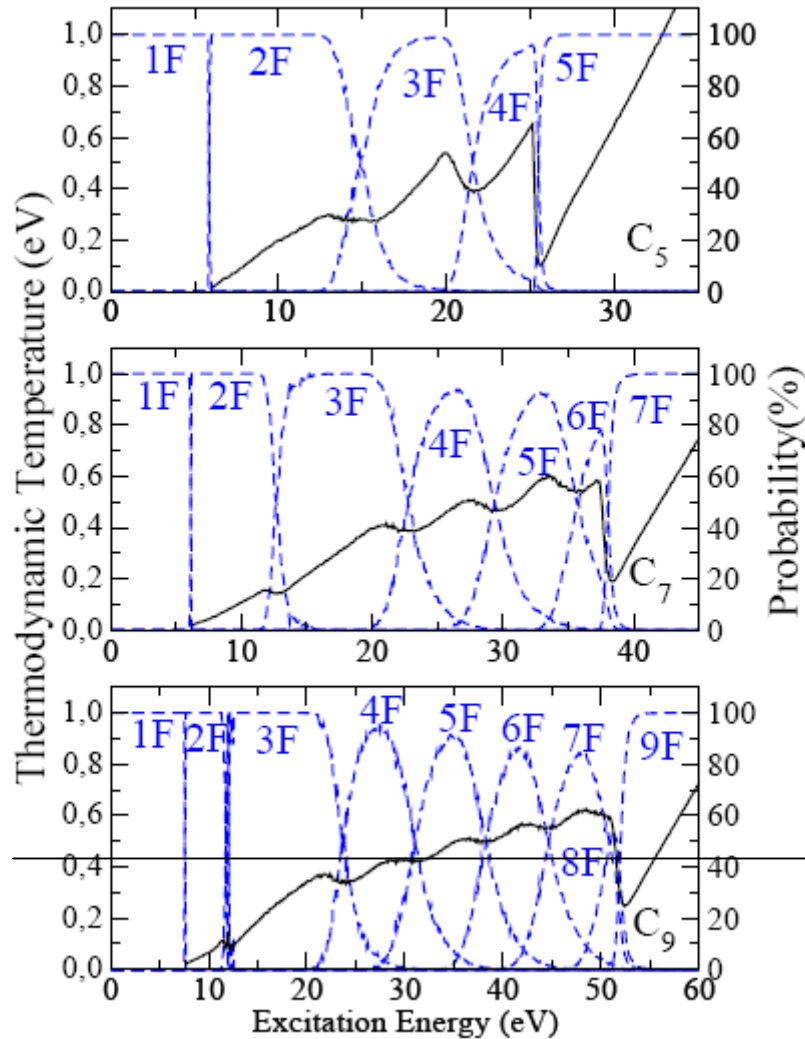


$$f(E) = NE^{a_1} \exp[-a_2(E - a_3)^{a_4}]$$

Same energy distributions !



Phase transition



$$\frac{1}{T} = \frac{\partial S}{\partial E_v^*} = \left\langle \frac{\alpha - 1}{E'_0} \right\rangle$$

$$E'_0 = E - (E_C + E_B + E_v^*) = K_t + K_r$$

$$\alpha = \frac{1}{2} \left(3N_f - 3 + \sum_{j=1}^{N_f-1} f_{rj} \right)$$

f_{rj} : number of rotational degrees of freedom

Boiling temperature of bulk carbon: **0.44 eV**

S. Diaz-Tendero et al., Phys. Rev. A 71, 033202 (2005).

Conclusions

- The formation of C_3 (linear) play a dominant role

Inclusion of several isomeric forms as well as rotational effects is essential to reproduce the experimental observations

- For CTMF good agreement with experimental measurements



**validation of our MMMC Fragmentation model
(for the first time in the field of atomic clusters!)**

**Combination of experimental measurements with accurate statistical
Fragmentation simulations can provide a reasonable estimation
of the cluster energy distribution just after the collision**



**Existence of a phase transition
(could be observed by increasing the impact velocity)**